

Clemson University

**TigerPrints**

---

All Theses

Theses

---

5-1985

## **A Study in Pervaporation of Ethanol/Water Mixtures and Its Applications to Membrane-Aided Distillation**

Mikel E. Goldblatt

Follow this and additional works at: [https://tigerprints.clemson.edu/all\\_theses](https://tigerprints.clemson.edu/all_theses)



Part of the **Chemical Engineering Commons**

---

5-1985

# A Study in Pervaporation of Ethanol/Water Mixtures and Its Application to Membrane-Aided Distillation

Mikel E. Goldblatt  
*Clemson University*

Follow this and additional works at: [https://tigerprints.clemson.edu/arv\\_theses](https://tigerprints.clemson.edu/arv_theses)

---

## Recommended Citation


Goldblatt, Mikel E., "A Study in Pervaporation of Ethanol/Water Mixtures and Its Application to Membrane-Aided Distillation" (1985). *Archived Theses*. 3307.  
[https://tigerprints.clemson.edu/arv\\_theses/3307](https://tigerprints.clemson.edu/arv_theses/3307)

This Thesis is brought to you for free and open access by the Theses and Dissertations at TigerPrints. It has been accepted for inclusion in Archived Theses by an authorized administrator of TigerPrints. For more information, please contact [kokeefe@clemson.edu](mailto:kokeefe@clemson.edu).

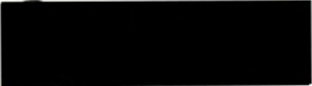
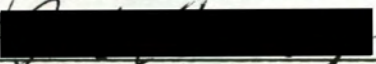
May 8, 1985

To the Graduate School:

Herewith is submitted a thesis written by Mikel E. Goldblatt entitled "A Study in Pervaporation of Ethanol/Water Mixtures and its Application to Membrane-Aided Distillation." I recommend that it be accepted in partial fulfillment of the requirements for the degree of Master of Science, with a major in Chemical Engineering.

  
\_\_\_\_\_  
Thesis Advisor

We have reviewed this thesis  
and recommend its acceptance:

  
\_\_\_\_\_  
  
\_\_\_\_\_

Accepted for the Graduate School:

  
\_\_\_\_\_

A STUDY IN PERVAPORATION OF ETHANOL/WATER  
MIXTURES AND ITS APPLICATION TO  
MEMBRANE-AIDED DISTILLATION

---

A Thesis  
Presented to  
the Graduate School of  
Clemson University

---

In Partial Fulfillment  
of the Requirements for the Degree  
Master of Science  
Chemical Engineering

---

by  
Mikel E. Goldblatt  
May 1985



## ABSTRACT

Pervaporation is a membrane separation process in which the permeate is flashed from the downstream side of the membrane into a low pressure stream. It may be used to separate close-boiling or azeotrope-forming mixtures at concentrations where reverse osmosis is infeasible.

In this study, an experimental pervaporation apparatus was constructed and pervaporation of ethanol/water solutions through a commercially available membrane was studied at various feed temperatures, permeate pressures, and feed compositions. The flux through the membrane, which was on the order of  $0.25 \text{ kmol}/(\text{m}^2\text{-hr})$ , increased at higher feed temperatures and also at lower permeate pressures. The selectivity for water permeation increased with ethanol concentration of the feed. Near the azeotrope the selectivity was about 1.4.

Membrane-aided distillation is a proposed process that uses pervaporation in conjunction with simple distillation to purify azeotropic solutions such as ethanol/water. A computer program was written to simulate the membrane-aided distillation process using the data from the pervaporation experiments and to optimize plant parameters for minimum cost. The cost of upgrading 82.5 mole percent ethanol to anhydrous ethanol was calculated to be about 53¢/gal of anhydrous ethanol produced which is roughly double the cost of the azeotropic distillation schemes now in commercial use. Using data from the

literature on a more selective, lower flux membrane, the simulation showed that this cost could be reduced to about 13¢/gal. These results indicate that with improvements in membrane selectivity, membrane-aided distillation may be an economically attractive process for the separation of azeotropes.



## VITA

Mikel E. Goldblatt was born June 24, 1956 in Philadelphia, PA. He enrolled at the University of Massachusetts at Amherst where he was a member of the American Institute of Chemical Engineers and Tau Beta Pi. He was granted a Bachelor of Science Degree in chemical engineering with a minor in chemistry in May 1983.

During the summer before his junior year, Mr. Goldblatt held a position with the Planning and Technical Services division of the Philadelphia Water Department. The summer before his senior year, he was employed by E. I. duPont de Nemours and Co. and was a member of the process engineering group at its Memphis petrochemicals plant. He enrolled at Clemson University in August 1983 to pursue a Master of Science degree in chemical engineering.

#### ACKNOWLEDGEMENTS

The author wishes to express his thanks to Dr. Charles H. Gooding, thesis advisor, for his helpful advice and discussion.

The author would like to express his appreciation to the Tennessee Valley Authority, the South Carolina Energy Research and Development Center, and the Allied Foundation for financial support of this work, and to the Universal Oil Products Company for supplying the membrane samples.

The author would also like to thank his family for their support and his colleagues for their comradeship.



## TABLE OF CONTENTS

	Page
TITLE PAGE .....	i
ABSTRACT .....	ii
VITA .....	iv
ACKNOWLEDGEMENTS .....	v
LIST OF TABLES .....	viii
LIST OF FIGURES .....	ix
 CHAPTER	
I. INTRODUCTION .....	1
II. LITERATURE REVIEW .....	3
Separation of Azeotropes .....	3
Membranes .....	5
Permeation Theory .....	6
Flux and Selectivity .....	10
Recent Experiments in Pervaporation of Ethanol/Water Solutions .....	14
Proposed Separation Schemes .....	16
III. EXPERIMENTAL .....	21
Plan of Experimentation .....	21
Method of Procedure .....	21
IV. EXPERIMENTAL RESULTS AND DISCUSSION .....	26
Permeation Rate .....	26
Selectivity .....	28
Limitations .....	31
Experimental Error .....	34
V. SIMULATION OF MEMBRANE-AIDED DISTILLATION .....	37
Plant Mass Balance Calculations .....	37
Plant Subunit Size and Cost Calculations .....	43



## Table of Contents (Cont'd.)

	Page
VI. SIMULATION RESULTS AND DISCUSSION .....	47
Simulation with the UOP-TFC801 Membrane .....	47
Inaccuracy in the Simulation .....	53
Simulation Using a More Selective Membrane .....	55
VII. CONCLUSIONS .....	58
VIII. RECOMMENDATIONS .....	59
APPENDICES .....	60
A. Pervaporation Laboratory Data and Results .....	61
B. Materials and Apparatus .....	64
C. Pervaporation Data Reduction Program Listing .....	69
D. Simulation Program Listing with Sample Output .....	75
E. Ethanol/Water Vapor-Liquid Equilibrium Data .....	91
F. Cost Correlations .....	94
G. Nomenclature .....	95
LITERATURE CITED .....	98

## LIST OF TABLES

Table	Page
I. Data Reported in Literature for Pervaporation of Ethanol/Water Mixtures .....	15
II. Simulation Chosen Variables and Constraints .....	44
III. Capital and Energy Costs as a Function of Pervaporator Feed to Permeate Ratio .....	54
A-I. Laboratory Data and Calculated Results for Constant Feed Composition Experiments .....	62
A-II. Laboratory Data and Calculated Results for Constant Feed Temperature and Permeate Pressure Experiments .....	63



## LIST OF FIGURES

Figure	Page
1. Schematic Diagram of Azeotropic Distillation Process .....	4
2. Illustration of Reverse Osmosis .....	7
3. Illustration of Pervaporation .....	7
4. Schematic Diagram of an Ethanol Dehydration Plant Using Two Membrane Units and One Distillation Column .....	17
5. Schematic Diagram of the Membrane-Aided Distillation Process .....	19
6. Illustration of Membrane-Aided Distillation Showing Typical Ranges of Operation .....	20
7. Schematic Diagram of Pervaporation Experimental Apparatus .....	22
8. Total Flux Through the Membrane as a Function of Permeate Pressure with Feed Temperature as a Parameter .....	27
9. Component Flux as a Function of Feed Composition .....	29
10. Separation Factor as a Function of Feed Composition .....	30
11. Permeate Composition as a Function of Feed Composition Compared with VLE Data for the Ethanol/Water System .....	32
12. Permeate Composition as a Function of Feed Composition Compared with VLE Data in the Neighborhood of the Azeotrope .....	33
13. Schematic Diagram of the Membrane-Aided Distillation Process with Overall Mass Balance Parameters .....	38
14. Flow Chart for Simulation Program .....	39
15. Column Subroutine Flowchart .....	40

## List of Figures (Cont'd.)

Figure	Page
16. Selected Stream Flows as a Function of $X_{FDP}$ .....	48
17. Capital and Energy Costs as a Function of $X_{FDP}$ .....	49
18. Total Upgrading Costs as a Function of $X_{FDP}$ with $X_{D2}$ , $F_{DP:P}$ as Parameters .....	50
19. Total Upgrading Costs as a Function of $X_{FDP}$ with $X_{D1}$ , $X_{D2}$ as Parameters .....	52
20. Total Upgrading Costs Using a More Selective Membrane .....	56
B-1. Diagram of Pervaporation Module .....	66
E-1. Vapor-Liquid Equilibrium Curve for the Ethanol/Water System at 1 Atmosphere .....	92
E-2. Vapor-Liquid Equilibrium Curve for the Ethanol/Water System Below 15 Mole Percent Water .....	93



## CHAPTER I

### INTRODUCTION

Many important industrial chemicals must be purified from azeotrope-forming mixtures. To separate such mixtures by distillation requires the addition of components which alter the relative volatility of the mixture for easier separation, but the additional components must be removed in subsequent steps. These separation systems are necessarily complex and often energy intensive.

In the last twenty-five years, the membrane separation techniques known as ultrafiltration and reverse osmosis have become commonly used in food processing, waste concentration, and desalination. Reverse osmosis, a pressure driven process, often may be applied successfully to concentrate a solute to perhaps 10 or 20 mole percent. However, concentration of a solute to high purity using reverse osmosis is not feasible due to the enormous osmotic pressure which opposes permeate flux.

Pervaporation is a modification of reverse osmosis that circumvents the osmotic pressure problem. The permeate is flashed to form a low-pressure vapor stream or into an unsaturated carrier gas. A proper membrane passes one component preferentially, and the permeate is quickly withdrawn from the downstream side of the membrane.

The primary purpose of this research was to design and build an experimental system to study the pervaporative separation of azeotropes. In particular, the flux and selectivity of ethanol/water



mixtures through a thin film composite membrane (UOP-TFC801) were to be investigated at varying conditions of feed temperature, permeate pressure, and feed composition.

The secondary goal of this investigation was to develop and apply empirical models of the pervaporation process to explore the economics of a membrane-aided distillation scheme for obtaining anhydrous ethanol from a dilute aqueous feed stream.

## CHAPTER II

### LITERATURE REVIEW

#### Separation of Azeotropes

Highly non-ideal mixtures often form azeotropes, wherein the equilibrium vapor and liquid compositions are identical. Azeotropy can lead to processing problems because simple distillation will not effect a separation of a mixture at azeotropic conditions. Ethanol, for example, is a widely used industrial chemical that is most often purified from an aqueous solution. Aqueous ethanol forms a minimum temperature azeotrope at 89.4 mole percent (95.6 mass percent) ethanol.

Azeotropic distillation is most commonly used to obtain pure (anhydrous) ethanol. In azeotropic distillation a third component is added to form a ternary azeotrope with the feed components, and the ternary azeotrope is removed as the overhead product (in the case of a minimum temperature azeotrope). Figure 1 depicts a typical azeotropic distillation process.

In the ethanol/water case, benzene is often the third component, or entrainer used. Referring to Figure 1, the benzene(B)/ethanol(E)/water(W) ternary azeotrope is removed overhead in the azeotropic column. The overhead stream is condensed and passes to a decanter where it separates into an organic layer containing only 1 mole percent water and a water layer containing 36 mole percent water (15). The organic layer is recycled to the azeotropic column where it begins the entrainment-of-water cycle again. The water layer is sent



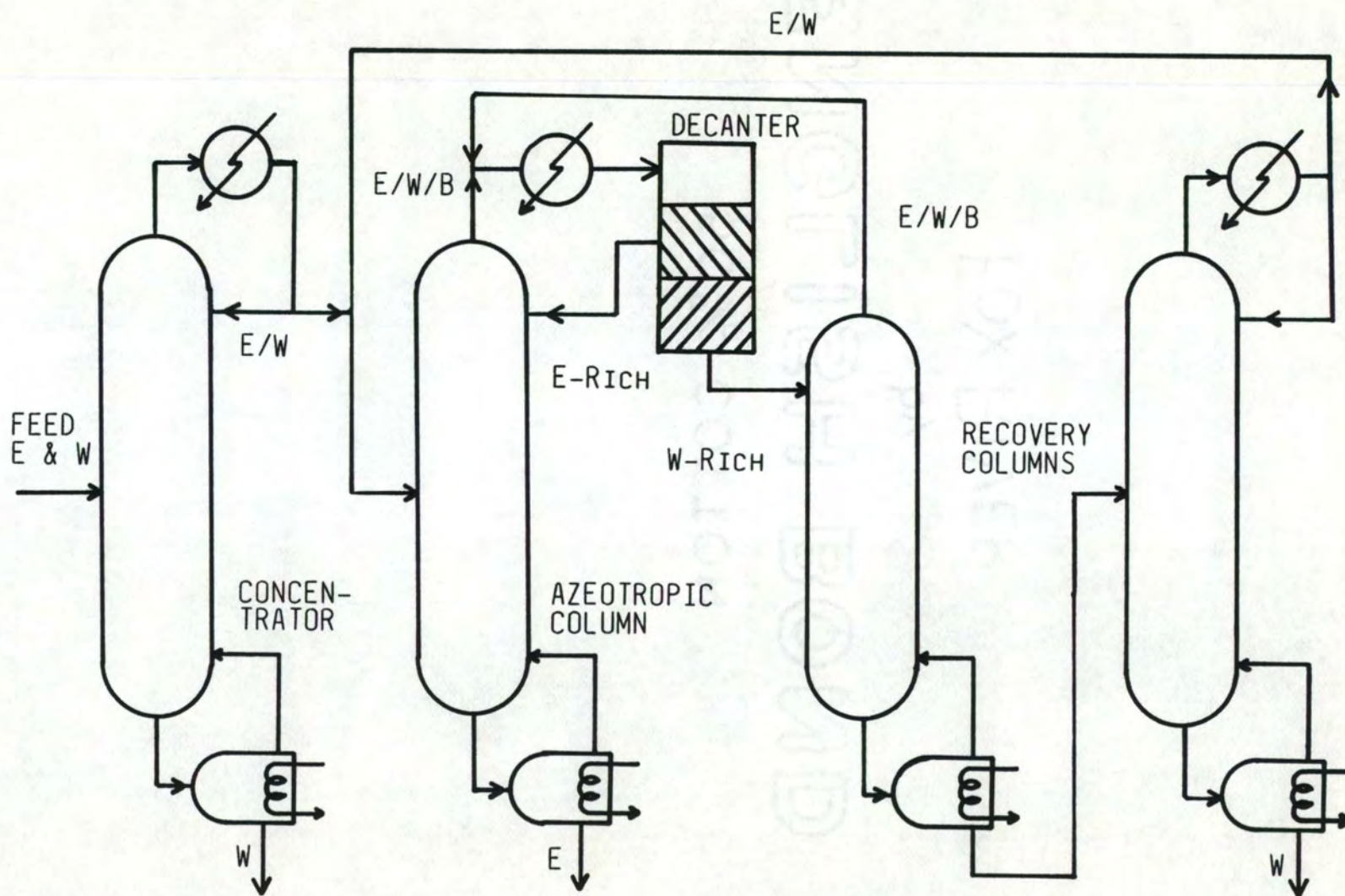


Figure 1. Schematic Diagram of Azeotropic Distillation Process



to a stripping column for removal of water as bottoms and recovery of benzene and ethanol in the form of the ternary azeotrope overhead. This overhead is condensed and sent to the decanter where it separates into two layers in the same manner as discussed for the azeotropic column overhead. Any ethanol leaving as bottoms from the stripping column is recovered by simple distillation and recycled as feed to the azeotropic column.

Azeotropic distillation is quite effective but does have some drawbacks. The process is energy intensive, employing four distillation columns. The entrainer used, often benzene for the ethanol/water separation, can create environmental problems if significant amounts are lost in the waste stream. Other methods have been used to alter the selectivity in vapor-liquid equilibrium of azeotropic systems. Generally these consist of adding salts or solvents to the system and removing the additional components in subsequent steps. Some are reported to be successful, but the benzene-based azeotropic distillation scheme is still the most widely used approach.

### Membranes

There is great incentive to explore alternative methods to purify ethanol and other azeotrope-forming systems. Membranes offer the possibility of effecting separations of azeotropes without the need of adding a third liquid component. The membrane itself acts as the third component, preferentially absorbing and diffusing one species, even at azeotropic conditions. Membrane separation also offers the possibility of purifying binary (and multicomponent) solutions at decreased energy demand. Reverse osmosis and pervaporation are the two membrane processes which will be discussed in the following paragraphs.



Reverse osmosis. Reverse osmosis (RO) through semi-permeable membranes has been widely used in the last 25 years in such functions as desalination and waste concentration. In this process a high pressure is applied to a feed stream in the presence of the membrane. The membrane preferentially passes one component so that the feed becomes enriched in the other component. RO typically employs pressure on the order of 100 atmospheres and is limited to fairly dilute systems. Figure 2 depicts a reverse osmosis system.

Pervaporation. Pervaporation (PVP) is a process which is similar to RO except that the range of pressures used is such that a phase change occurs on the downstream or permeate side of the membrane. The permeate side is maintained below the saturated vapor pressure of the permeate so that the permeate is flashed from the membrane surface. Pervaporation pressures are typically atmospheric upstream and on the order of 0 to 250 mmHg absolute downstream. Pervaporation is applicable to separations over the entire composition range. Figure 3 depicts a pervaporation system.

#### Permeation Theory

The following section presents the governing principles of permeation through semi-permeable membranes and compares reverse osmosis with pervaporation. For more detailed development of the governing equations, see references (12,13,26).

Driving force. If we look at the membrane as a black box, for the moment, we may speak of a driving force between the upstream bulk fluid and the downstream bulk fluid, knowing that this driving force



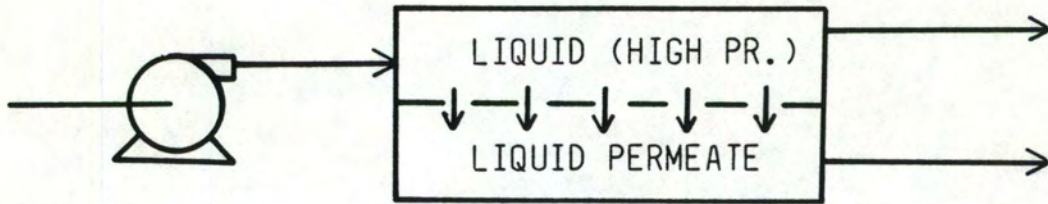


Figure 2. Illustration of Reverse Osmosis.

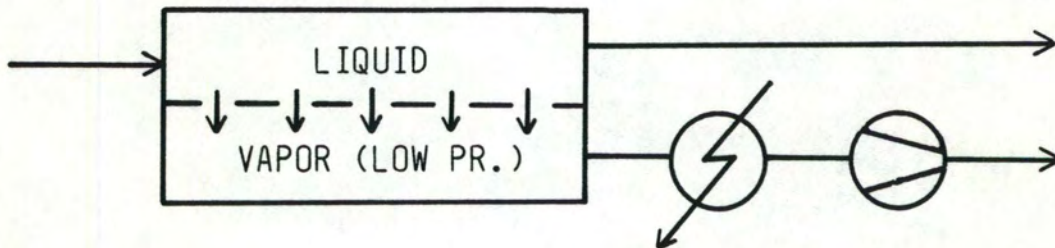


Figure 3. Illustration of Pervaporation

must be present to have a net flux through the membrane. The driving force for permeation may be expressed as the difference in chemical potential between the fluids. Representing upstream and downstream with subscripts 1 and 2, we may express the chemical potential of the permeating species  $i$  as a function of pressure and concentration. For an isothermal system with incompressible fluids,

$$\mu_{1i} = \mu_{i0} + v_{1i} (P_1 - P_{\text{ref}}) + RT \ln a_{1i}, \quad (1)$$

$$\mu_{2i} = \mu_{i0} + v_{2i} (P_2 - P_{\text{ref}}) + RT \ln a_{2i} \quad (2)$$

where

$\mu_{1i}, \mu_{2i}$  = chemical potential of permeating species,

$\mu_{i0}$  = the chemical potential of pure liquid  $i$  at  $T$  and  $P_{\text{ref}}$ ,

$v_i$  = molar volume of species  $i$ ,

$a_i$  = activity of species  $i$ ,

$R$  = universal gas constant,

$T$  = absolute temperature,

$P$  = pressure upstream or downstream,

$P_{\text{ref}}$  = an arbitrary reference pressure.

The driving force across the membrane is then expressed as a difference in chemical potential as follows:

$$\Delta\mu_i = \mu_{1i} - \mu_{2i}. \quad (3)$$

Reverse osmosis. For convenience, we may choose  $P_{\text{ref}} = P_2$ . Then combination of equations (1), (2), and (3) gives

$$\Delta\mu_i = v_{1i} (P_1 - P_2) + RT \ln \left( \frac{a_{1i}}{a_{2i}} \right). \quad (4)$$



For the two liquid phases we may express the activities in terms of activity coefficients so that equation (4) becomes

$$\Delta\mu_i = v_{1i} (P_1 - P_2) + RT \ln \left( \frac{\gamma_{1i} x_{1i}}{\gamma_{2i} x_{2i}} \right) \quad (5)$$

where

$x_i$  = liquid mole fraction of component  $i$ ,

$\gamma_i$  = activity coefficient of component  $i$ .

The second term on the right side of equation (5) will be negative for an ideal solution in which the component  $i$  passes through the membrane preferentially. This negative driving force term must be overcome by the first term on the right side in order to have any net driving force for permeation. The second term is often expressed in terms of osmotic pressure which may be described as that pressure necessary to offset the concentration gradient in order to attain equilibrium. For an osmotic system at equilibrium,  $\Delta\mu_i = 0$ . Equation (4) then may be rearranged to express the osmotic pressure,  $\pi_i$ , as

$$\pi_i = (P_1 - P_2) = \frac{-RT}{v_{1i}} \ln \left( \frac{\gamma_{1i} x_{1i}}{\gamma_{2i} x_{2i}} \right) . \quad (6)$$

Since the osmotic pressure becomes very large as the mole fraction ratio decreases, reverse osmosis is limited to fairly modest concentration of dilute feeds.

Pervaporation. In pervaporation there is a phase change and a low pressure is maintained downstream. It is more convenient in this case to let  $P_{ref} = P_i^s$ , the saturated vapor pressure of component  $i$ . Since the downstream phase is vapor, the term  $v_{2i}(P_2 - P_{ref})$  disappears from equation (2). Since the downstream pressure is low, we may assume



ideal gas behavior and represent the activity for the permeate as follows:

$$a_{2i} = \frac{y_{2i}P_2}{P_i^s} \quad (7)$$

where

$y_i$  = vapor mole fraction of component  $i$ .

Combining equations (1), (2), (3), and (7) and again using the activity coefficient for the liquid feed, we can represent the driving force for pervaporation as follows:

$$\Delta\mu_i = v_{1i} (P_1 - P_i^s) + RT \ln \left( \frac{\gamma_{1i} x_{1i} P_i^s}{y_{2i} P_2} \right) . \quad (8)$$

If we keep  $P_2$  small, both of the terms on the right side are positive with the second term dominating. This illustrates the applicability of pervaporation to separations in any composition range.

#### Flux and Selectivity

Many researchers (5,17,31) describe membrane separations through thin film polymer membranes by use of a solution-diffusion model. The three steps which describe the solution-diffusion mechanism of membrane permeation are:

1. dissolution of the feed liquid into the membrane,
2. diffusion through the membrane,
3. evaporation of permeate from the downstream face.

The membrane selectivity is caused both by differences in solubilities of the respective components in the membrane polymer and by differences in the diffusivities of component permeants through the polymer film. In general, solubility differences result from varying degrees of interaction between the components of the solution and

functional groups on the membrane. The popular cellulose acetate and polyamide membranes contain active hydroxyl and amine groups. Aptel et al. (1) have experimented with the grafting of very thin films of polymer groups onto membranes. These groups preferentially absorb one component of a feed mixture. For instance, experiments with the grafting of N-vinylpyrrolidone (VP) onto poly(tetrafluoroethylene) films (PTFE) yielded results which showed enhanced flux for components which form hydrogen bonds with the VP group.

Steady state diffusion through a membrane may be described by Fick's Law of diffusion. For component  $i$ ,

$$J_i = -D_c \frac{dc_i}{dz} \quad (9)$$

where

$D_c$  = diffusion coefficient (concentration dependent),

$c_i$  = concentration of species  $i$  in polymer film,

$z$  = distance into polymer film measured from feed side.

For a membrane of finite thickness,  $L$ , equation (9) may be integrated from  $z = 0$  to  $z = L$  to get

$$J_i = -\frac{1}{L} \int_{C_{i,z=0}}^{C_{i,z=L}} D_c dc_i. \quad (10)$$

Huang and Jarvis (17) have further refined this expression for the case of permeation at very high vacuum downstream and the assumption of equilibrium sorption at the membrane feed side. At low downstream pressure,  $C_{i,z=L} = 0$ . At equilibrium sorption on the feed side,  $C_{i,z=0}$  may be expressed in terms of solubility of liquid in the



polymer,  $C_{i,s}$ . Equation (10) then becomes

$$J_i = \frac{1}{L} \int_0^{C_{i,s}} D_c dc_i \quad (11)$$

where it is now explicit that component flux is a function of solubility in the polymer and diffusion through the polymer.

Diffusivity through the polymer film is often expressed as a concentration-dependent Arrhenius-type relation as follows:

$$D_c = D_{oi} e^{b_i c_i} \quad (12)$$

where

$D_{oi}$  = diffusion coefficient at dilute conditions,

$b_i$  = an empirical constant.

Power law models have also been proposed (38) to describe diffusivity through polymer membranes.

The plasticizing action of certain feed components such as water has an important effect on permeation rate and selectivity. Plasticizing may be described as the swelling of amorphous polymer regions. This swelling results in higher mobility of polymer chain segments and easier passage through the membrane. Huang and Jarvis (17) have demonstrated the plasticizing effect of water on the permeability of polyvinyl alcohol membranes. Increased concentration of water in the feed was found to enhance fluxes and decrease selectivity (17). It has also been proposed (1,17) that a component's self-affinity may lead to a clustering effect which decreases flux but increases selectivity.



Paul and Paciotti (31) have examined flux data and found that at low concentration of permeant in the polymer film, diffusivity generally follows a concentration dependence as expressed in equation (12). However for moderately concentrated solutions in the polymer and highly swollen polymer membrane networks, they found that over a considerable range diffusivity was virtually independent of concentration.

Membrane thickness. Again examining Fick's Law, equation (10), one can see that the permeation rate of any species should be inversely proportional to the membrane thickness,  $L$ . Thus, decreasing the membrane thickness increases flux without changing selectivity. Various experimenters (1,5) have found this to be the case. Therefore, for high flux, thinner membranes are generally preferred.

Temperature effects. Huang and Jarvis (17) explain temperature effects using Eyring's hole theory of diffusion. At higher temperatures, thermal motion of the polymer chains increases, producing larger diffusive holes, thus increasing flux and decreasing selectivity. However, other researchers (1,3) have observed increased flux with relatively no effect on selectivity at increased temperatures.

Pressure effects. In pervaporation, decreased downstream pressure decreases the activity of the permeate which increases the driving force for permeation. With decreased permeate pressure, flux generally increases. Selectivity at decreased permeate pressure has been found to increase for some systems and decrease for others (3). According to the work of Shelden and Thompson (38) selectivity is determined by intrinsic membrane properties at very low permeate



pressure but is influenced primarily by relative volatility as the permeate approaches saturation.

The parameters which influence flux and selectivity are summarized below. Although different membranes behave differently, some general trends can be observed:

- i) Higher feed temperatures will generally yield higher fluxes. Selectivity may decrease or remain the same.
- ii) Feed pressure has little effect on pervaporation.
- iii) Lower permeate pressure will generally increase the flux and may affect the selectivity.
- iv) Feed composition may affect the selectivity and flux, with the trend of behavior depending on the membrane used.
- v) Membrane composition and structure are important parameters. The flux and selectivity obtained with a given feed mixture is influenced strongly by choice of polymers. Thinner membranes generally yield higher fluxes.

#### Recent Experiments in Pervaporation of Ethanol/Water Solutions

Various researchers (1,2,4,7,25,37,39) have experimented with pervaporation of ethanol/water solutions in order to obtain pure (anhydrous) ethanol. Table I shows some results of these researchers. The flux is given in terms of kmol/hr of permeate per square meter of membrane. Selectivity is expressed in terms of the separation factor,  $\alpha$ . The separation factor is analogous to relative volatility and is defined as

$$\alpha_{ij} = \frac{y_i/x_i}{y_j/x_j} = \left(\frac{y_i}{1-y_i}\right) \left(\frac{1-x_i}{x_i}\right) \quad (13)$$

where

$y$  = permeate mole fraction,

$x$  = feed mole fraction.

TABLE I. Data Reported in Literature for Pervaporation of Ethanol/Water Mixtures

Mass % EtOH in		Mole % EtOH in		Feed Temp (°C)	Permeate Pressure (mmHg)	Flux $\left(\frac{\text{kmol}}{\text{m}^2\text{-hr}}\right)$	Separation Factor	Membrane Type	Ref
Feed	Permeate	Feed	Permeate						
0.45	0.088	0.24	0.036	80	*	0.102	8.5	Cellulose Acetate	(4)
0.956	0.882	0.895	0.745	25	*	0.056	2.9	PTFE-PVP	(1)
0.959	0.748	0.901	0.537	43	0.08	0.030	7.9	RC100-UOP Polyetherurea	(37)
0.956	0.784	0.895	0.587	20	*	0.029	6	PTFE-PVP 65% grafting	(2)
0.956	0.784	0.895	0.587	55	*	0.049	6		
0.958	0.68	0.90	0.45	60	20	0.016	11	Unswollen Cellulose 2.5 Acetate	(28)
0.937	0.889	0.853	0.758	43	0.30	0.038	1.5	UM05 Amicon	(37)

\* Permeate pressures not given.



Subscript  $i$  represents the preferred permeating species (water in this case).

#### Proposed Separation Schemes

Flux vs. selectivity. Researchers have usually found (1,29,37) that there is a trade-off between flux and selectivity of a particular membrane. Generally there is an inverse relationship. Therefore any attempt to design an optimum system employing pervaporation must take this trade-off into account. For this reason, various multistage or multipass schemes (16,27,29,39) and some schemes which couple the membrane system with distillation units (11,23) have been proposed.

Tusel and Ballweg (39) have proposed a design which couples a multi-stage membrane separation system with a single concentration still to obtain pure ethanol from an aqueous ethanol feed. Highly selective, relatively low flux membranes are employed. The advantage of this system is that only one still is used instead of the four used in azeotropic distillation. However, the membrane area is necessarily large and two different membranes are used, a coarse split membrane and a finer finishing membrane. Figure 4 depicts this separation scheme. The Tusel group is actively developing this technology and the membranes to support it.

Gooding and Bahouth (11), on the other hand, have proposed a single stage membrane system coupled with two simple binary stills to effect a separation using a high flux, relatively low selectivity membrane. Here the advantage lies in the simplicity of the membrane system which uses the membrane to achieve only a coarse split of the azeotrope at high permeation rates, allowing the finishing still to



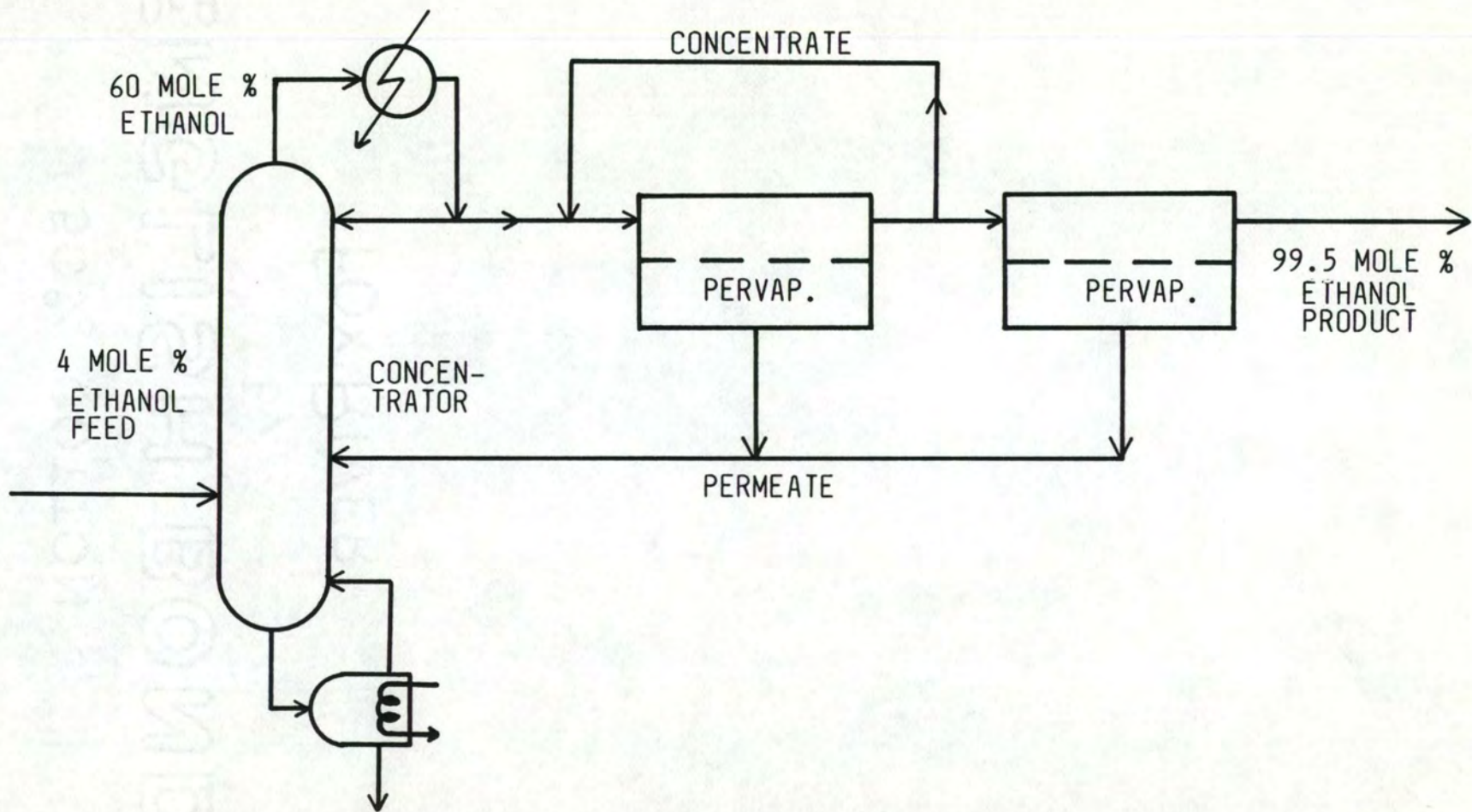


Figure 4. Schematic Diagram of an Ethanol Dehydration Plant Using Two Membrane Units and One Distillation Column



complete the purification. Figure 5 depicts this separation scheme. In this process the minimal membrane requirement is that the composition of the concentrate from the pervaporator must be on the ethanol-rich side of the azeotrope and the composition of the permeate must be on the water-rich side of the azeotrope. This is illustrated in Figure 6. Gooding and Bahouth have suggested that existing reverse osmosis membranes might be capable of providing sufficient selectivity to make this scheme economically attractive.

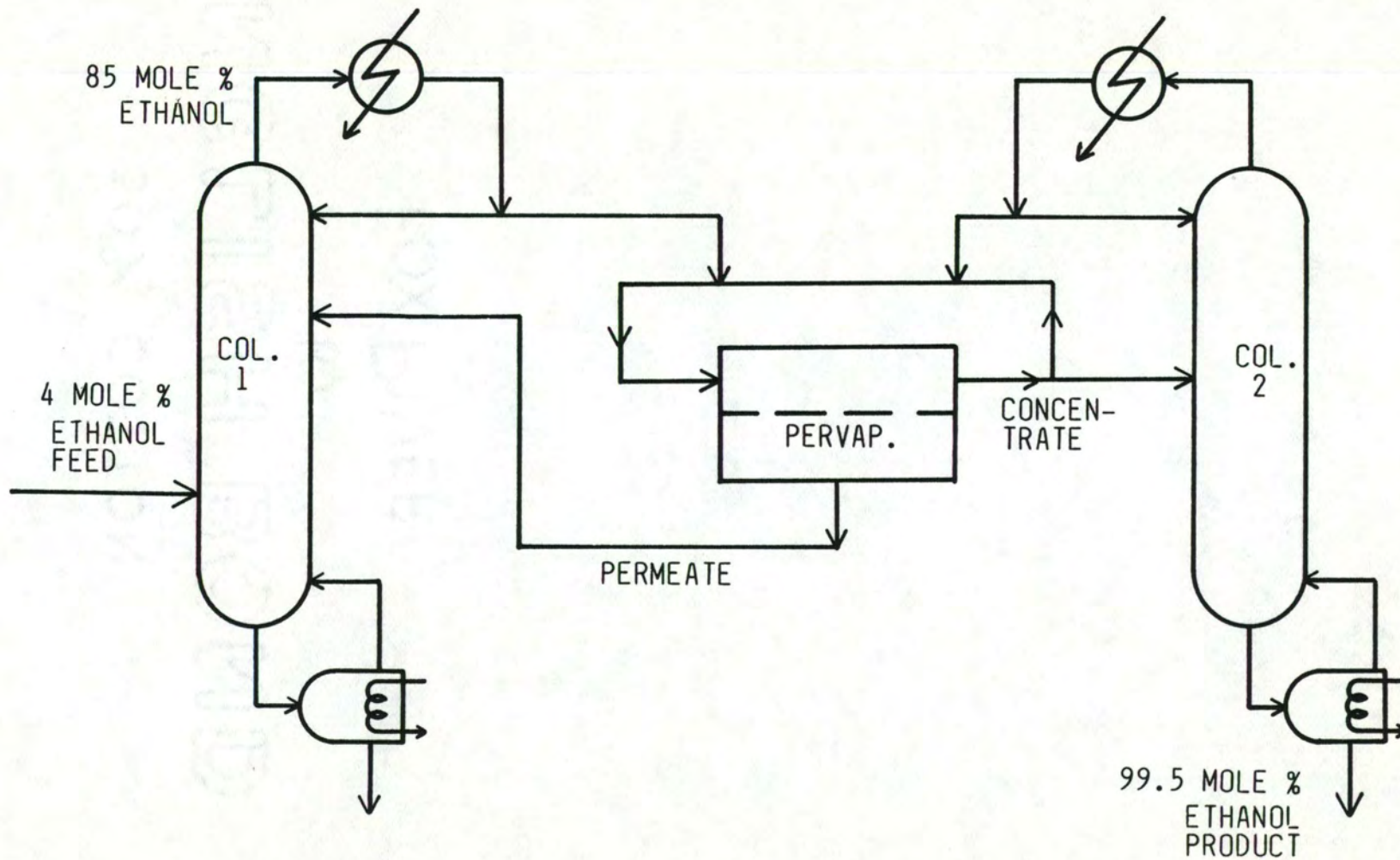


Figure 5. Schematic Diagram of the Membrane-Aided Distillation Process



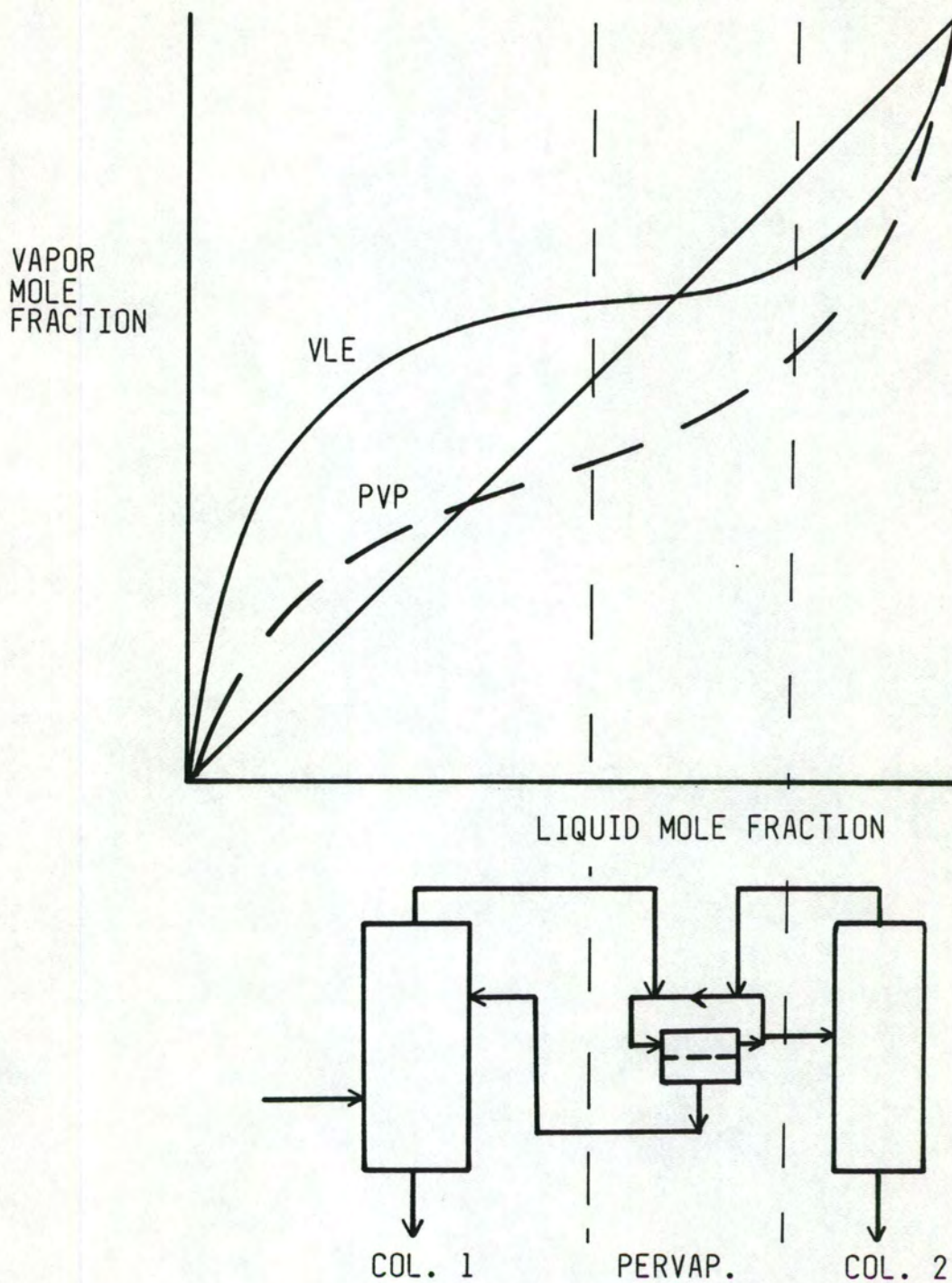


Figure 6. Illustration of Membrane-Aided Distillation Showing Typical Ranges of Operation



## CHAPTER III

### EXPERIMENTAL

#### Plan of Experimentation

The experimental portion of this investigation was undertaken to study certain controllable parameters in pervaporation of ethanol/water mixtures through a thin film composite membrane. The UOP-TFC801 membrane was chosen because it is produced domestically; it is available commercially; and in the reverse osmosis mode of operation, it has been found to permit a high permeation rate while still providing an adequate separation of ethanol/water mixtures (23).

The flux and selectivity were examined while varying the feed temperature and composition and the permeate pressure. Data were first collected at a constant, near-azeotropic feed composition, varying the feed temperature and the permeate pressure. Data were then collected at constant feed temperature and permeate pressure, varying the feed composition.

#### Method of Procedure

The following experimental procedure refers to the apparatus depicted in Figure 7.

Pre-startup. Before beginning an experimental run, a membrane was installed in the membrane module and the module was connected in the system as shown in Figure 7. (The module is described in more detail in Appendix B). All valves were closed. Five to 15 liters of an ethanol/water mixture of desired composition were charged to the feed tank.



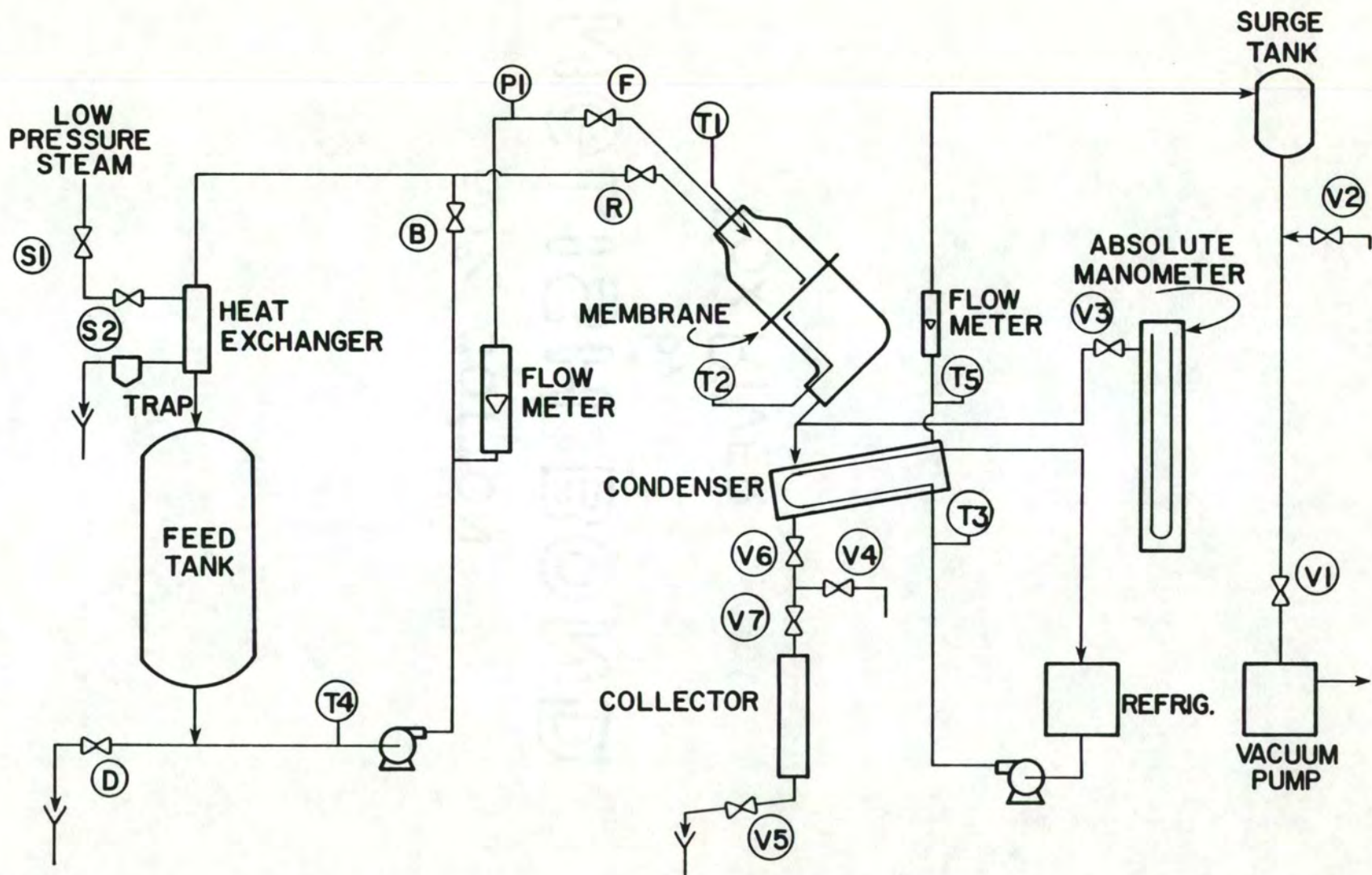


Figure 7. Schematic Diagram of Pervaporation Experimental Apparatus

Startup. The feed was heated to desired temperature and mixed by opening bypass valve B, turning on the feed pump, and opening steam valves S1 and S2. A sample of the feed was taken via valve D for analysis. The pump supplied a flow rate of about 8 /min, providing moderately turbulent flow across the surface of the membrane. The condenser was activated by first opening the valve (not pictured) providing cooling water to the refrigeration unit and then turning on the refrigerant circulation pump and the refrigeration unit. The vacuum system was activated by first turning on the vacuum pump, and then opening valves V1, V3, V6, and V7 in order to evacuate the permeate side of the system.

To begin an experimental run, the following procedure was used. When the feed reached the desired temperature as indicated by the recycle stream's temperature indicator, the feed and recycle valves to the membrane unit, F and R, were opened. The bypass valve, B, was then closed. Adjustments to maintain the desired temperature were made by turning steam valve S2. Valve V2 was opened to allow the permeate pressure to rise to the desired value. The permeate pressure was maintained by adjusting needle valve V2, a controlled leak.

Running an experiment. The system was first allowed to reach steady state as evidenced by constant pressure and temperature readings and a constant rate of permeate collection. Experimental and ambient conditions affected the length of time required to achieve steady state. Generally it was on the order of one hour.

The permeation rate was determined by measurement of the height of liquid in the collector versus time. Later a correction from the



reading on the purge stream flowmeter was applied to account for vapor losses. The height of liquid in the collector and the reading from the vapor flow meter were recorded at regular intervals. Also all temperature and pressure readings were recorded. Adjustments were made periodically to valve S2 to keep the feed temperature constant. Permeate pressure was also held constant for each particular run by adjustment of valve V2.

Taking samples. Since the feed flowrate was very large compared to the permeate flowrate and the feed was recycled to achieve the mixed tank effect, the feed composition changed very little during a single run. Samples for laboratory analysis were withdrawn periodically from valve D with virtually no upset to the system.

The permeate was sampled through a sample port located just above valve V7. Valve V7 was closed and left closed until enough liquid permeate accumulated to cover the sample port. Valve V6 was then closed and V4 opened slightly to provide pressure for withdrawal of a sample. A syringe was used to withdraw a measured sample, which was stored for laboratory analysis. Valve V4 was then closed and V7 opened to allow liquid permeate to again fall into the collector. Valve V6 was then slowly reopened to restore the system to routine operation. This sampling procedure interrupted the steady-state nature of the experiment for a minute or two as indicated by a pressure rise on the permeate side when valve V6 was opened. After the sample was taken, subsequent readings of the permeation rate were made to insure that the system returned to the desired condition.

Shutdown procedure. To shut down the system, the steam valves S2 and S1 were closed, the feed pump was turned off, and the bypass valve B was opened. Valves F and R were then closed. Next the refrigerator, coolant pump, and vacuum pump were turned off. The permeate collector was drained by opening valves V4 and V5. The system was then closed by closing valves V1 through V7. Cooling water for the refrigerator was turned off.

Sample analysis. Samples of feed and permeate were analyzed for water content by use of a Fischer titrimeter. Standard procedures for Fischer titration may be found in the ASTM Standards manual (30) or in manufacturers' literature.



## CHAPTER IV

### EXPERIMENTAL RESULTS AND DISCUSSION

The UOP-TFC801 membrane was employed to separate ethanol/water mixtures with feed temperatures ranging from 37.5 to 47.5°C permeate pressures of 30 to 70 mmHg absolute, and feed compositions ranging from 12.5 to 99.5 mole percent ethanol (0.5 to 87.5 mole percent water). Note that in this section concentrations will be expressed in terms of mole fraction of water. The following sets of parameters were correlated:

1. permeate flux as a function of feed temperature and permeate pressure at near-azeotropic feed compositions,
2. component flux versus feed composition,
3. permeate composition as a function of feed composition at constant temperature and pressure.

#### Permeation Rate

The permeation rate was found to be a function of feed temperature and permeate pressure. A plot of flux versus permeate pressure at various feed temperatures appears in Figure 8. This represents the general trend of increased flux at both increased feed temperature and decreased permeate pressure. The higher flux at higher temperature may be attributed to the increased motion of the polymer chains creating larger diffusive holes. For diffusion as the limiting step in permeation, this would have the most pronounced effect. Also, the sorption of the feed into the active polymer sites may have become more prominent due to higher solubility of the feed

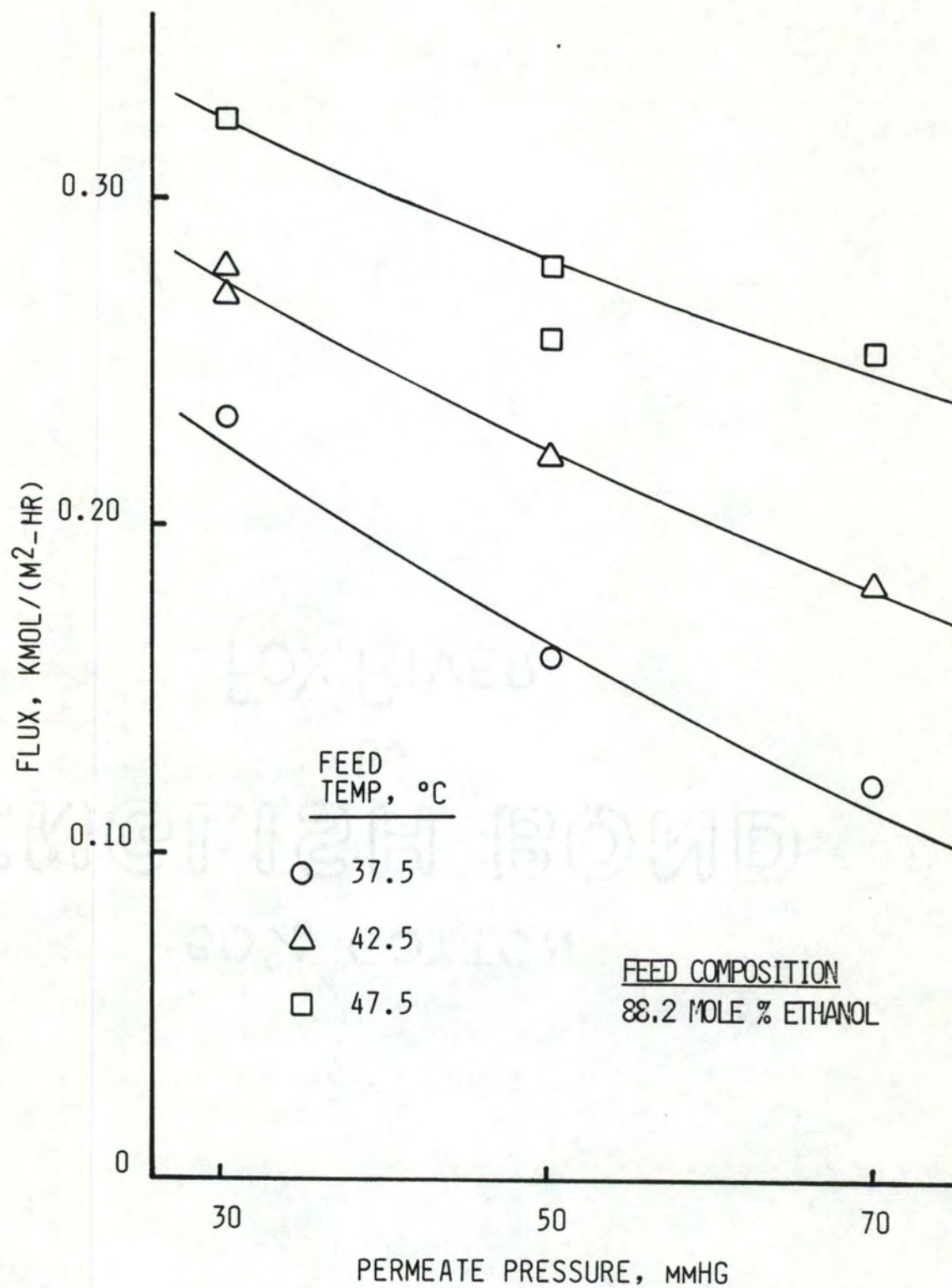


Figure 8. Total Flux Through the Membrane as a Function of Permeate Pressure with Feed Temperature as a Parameter



in the polymer. Lower permeate pressure increased flux due to the increased driving force. A model was fitted to the flux data with an exponential term for the permeate pressure driving force and an added linear temperature and pressure correction term. The equation for the model follows:

$$G_{TOT} = 1.39E-4 \exp [(0.0104)(760-P_2)] + C_T \quad (14)$$

where

$$C_T = \frac{T_1 - T_{ref}}{100} \left[ 1 + \frac{1}{120} (P_2 - P_{ref}) \right],$$

$$T_{ref} = 42.5 \text{ } ^\circ\text{C},$$

$$P_{ref} = 30 \text{ mmHg}.$$

#### Selectivity

Component fluxes are plotted in Figure 9 against mole fraction of water in the feed at constant feed temperature ( $T_1 = 42.5 \text{ } ^\circ\text{C}$ ) and permeate pressure ( $P_2 = 30 \text{ mmHg}$ ). Two curves are drawn through the data points in order to establish the smoothed trend of the separation factor. Figure 10 shows that the separation factor is a linear function of the feed composition. At the lowest feed water compositions the separation factor is quite sensitive to the placement of the smooth curves in Figure 9. Therefore the observed linear behavior of the separation factor is more speculative below 10 percent water. Azeotropic feeds yielded a separation factor of about 1.4. Below 35 percent water the membrane passed ethanol preferentially.

An alternative representation of the selectivity can be obtained by plotting permeate composition versus feed composition (the actual

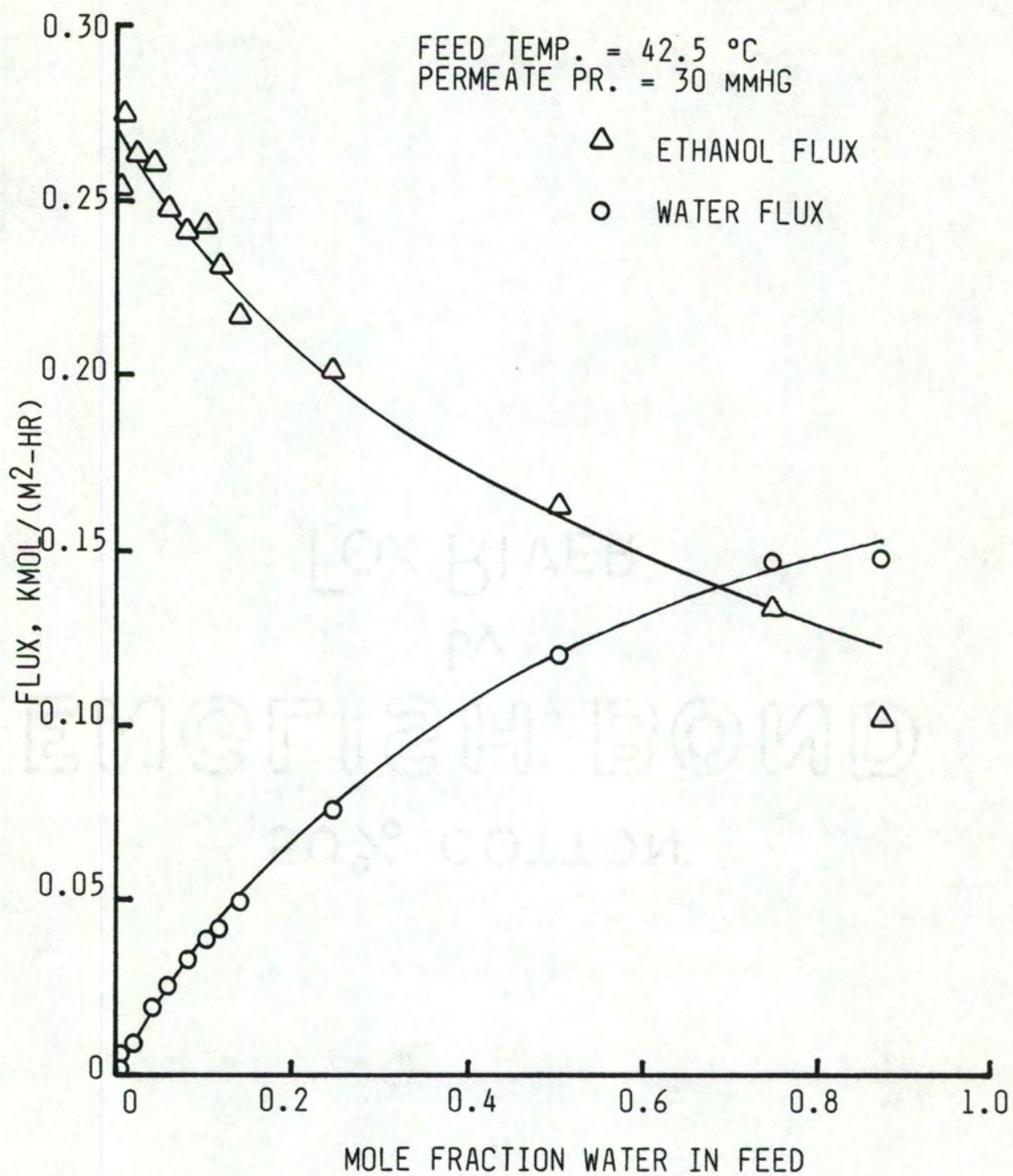


Figure 9. Component Flux as a Function of Feed Composition



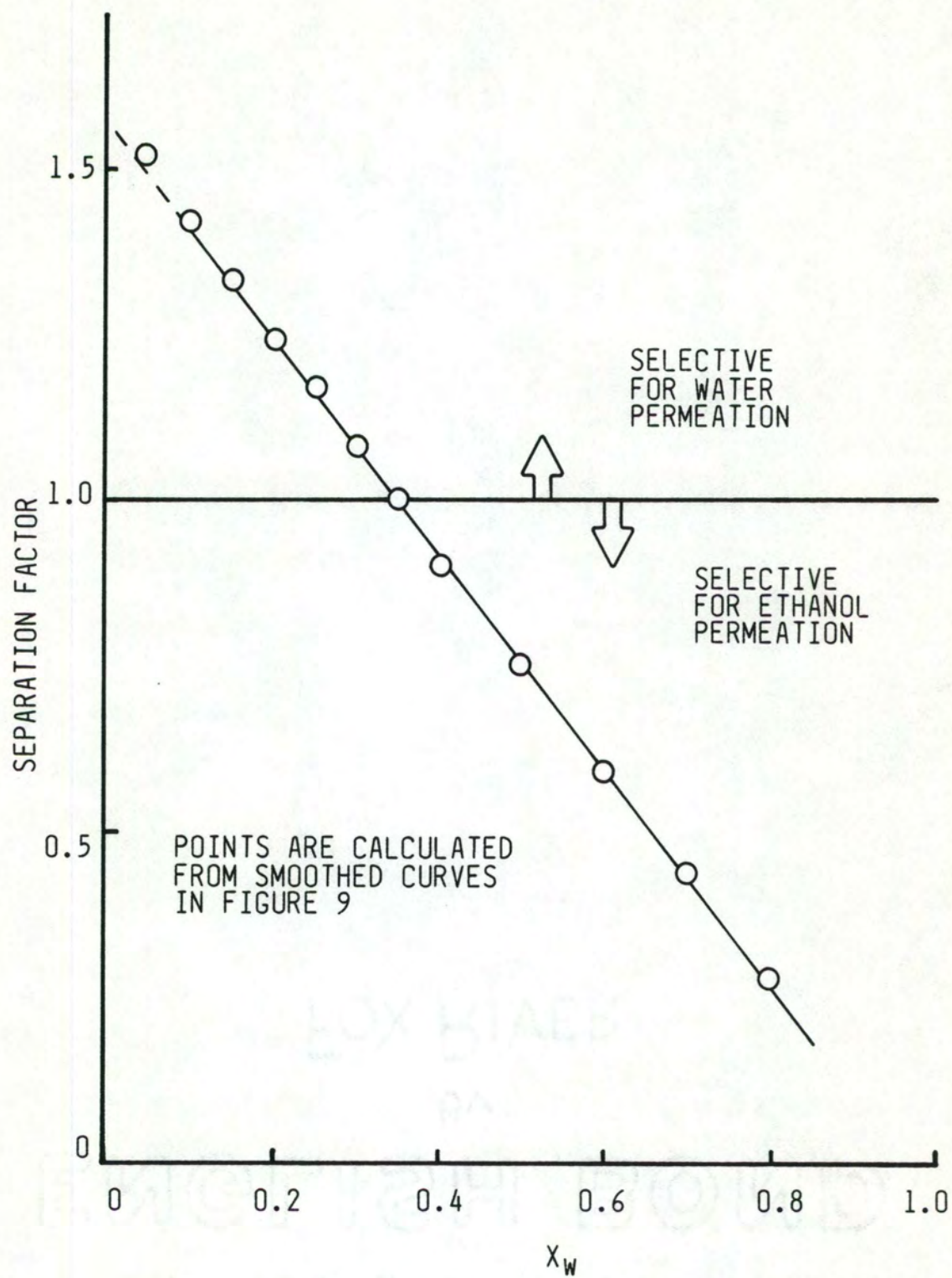


Figure 10. Separation Factor as a Function of Feed Composition

laboratory data) along with the vapor-liquid equilibrium data (Figure 11). Here it is apparent that the pervaporation curve follows the general shape of the equilibrium curve. This high flux membrane affords a modest increase in water passage over that which the equilibrium curve predicts through the entire range of composition. This implies a highly passable membrane, perhaps a very open polymer network, with modest selectivity occurring. A power law model was fitted to the data in the low range of water content. Figure 12 shows the experimental data points along with the model drawn in as a solid curve. The equation for the model follows:

$$y_w = mx_w^b \quad (15)$$

where

$$m = 0.791,$$

$$b = 0.776.$$

For the near-azeotropic mixtures, the separation factor was found to vary at different temperatures and pressures from about 1.2 to 1.6. However, there were no consistent trends so these results are not conclusive. The factors which may have contributed to variation in selectivity include variations in component solubility in and diffusivity through the membrane, membrane swelling, polymer motion, competition for sorption sites, and clustering effects.

#### Limitations

Physical limitations existed which restricted the range of experimental conditions and thus the range of data available.

The UOP-TFC801 membrane was rated by the manufacturer to withstand temperatures only as high as 50°C. Fluxes dropped



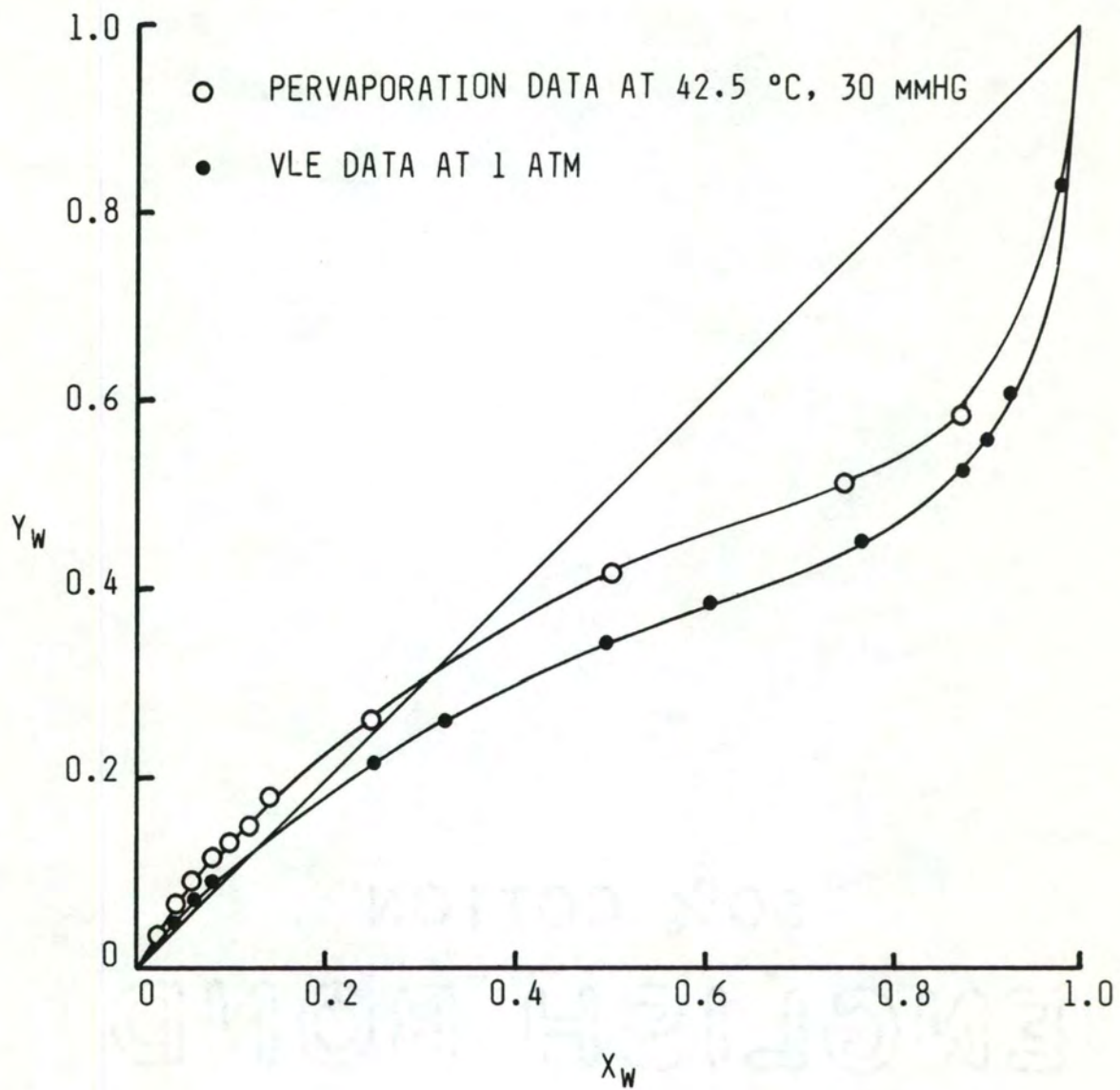


Figure 11. Permeate Composition as a Function of Feed Composition Compared with VLE Data for the Ethanol/Water System

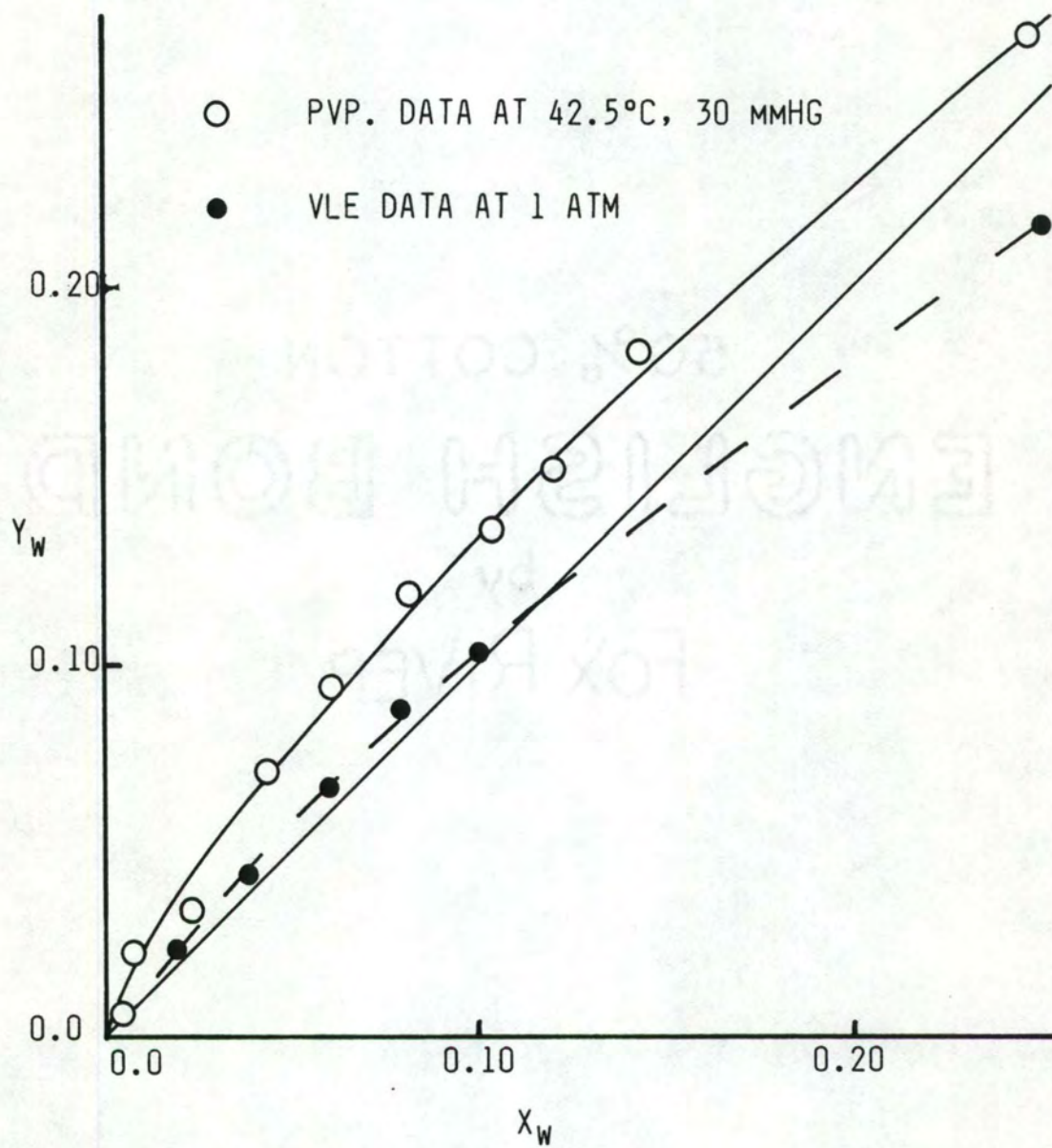


Figure 12. Permeate Composition as a Function of Feed Composition Compared with VLE Data in the Neighborhood of the Azeotrope



at lower temperatures so that the experimental temperatures spanned a range of only 10°C.

Other researchers have conducted pervaporation experiments at very low permeate pressures, necessitating the use of cold traps at liquid nitrogen temperatures to collect the permeate. Since the UOP-TFC801 membrane affords a relatively high flux, it was deemed unnecessary to go to the very low pressures. A refrigerated condenser was used to collect the permeate and permeate pressures ranged from 30 mmHg to 70 mmHg absolute.

#### Experimental Error

Of the possible sources of error, the most important involved permeate vapor passing through the condenser and being lost to the atmosphere via the vacuum pump. Sources of random error included small variations in the feed temperature, condenser temperature, and permeate pressure that could have influenced the results of a particular run, and the possibility of sampling and sample analysis error.

Permeate vapor lost. Since the refrigerant was circulated at 0 to 5°C, the temperature of the purge gas leaving the condenser was approximately 10°C. If leakage had been sufficiently low, this temperature was low enough to condense virtually all of the permeate. But air leakage did exist on the low pressure side of the system and at the lower permeate pressures, a significant amount of permeate vapor could escape condensation and exit the system via the vacuum pump. The amount of permeate vapor lost was determined by measurements of the flow rate of the purge stream. This amount was almost



always less than 10 percent of the total permeate flux. A correction was applied to account for this amount lost in the subsequent flux and selectivity calculations.

The vapor lost was assumed to be in equilibrium with the condensed liquid. The overall composition of the purge gas was calculated by assuming that the gas consisted of air saturated with the equilibrium ethanol/water mixture. The purge stream flow rate was measured by a Brooks rotameter with an applied correction from calibration conditions. During the course of an experimental run, the flow rate sometimes fluctuated by as much as 20 percent, indicating a source for experimental error. This error was minimized by taking frequent rotameter readings and using the average value for vapor flow calculations.

Other sources of error. All other sources of error were probably minor in comparison to the vapor loss error. Feed temperature during a particular run was controlled to within one or two °C, and permeate pressure to within 1 mmHg.

Samples were withdrawn from the feed tank and the permeate sample port. Since the feed tank was well mixed, little error was introduced in sampling the feed. Sampling of the permeate was done only after the system had sustained steady state operation for an hour, thus assuring withdrawal of a typical sample. Analysis of the samples was done by use of a Fischer titrimeter, where accuracy was attained in the neighborhood of one percent of the existing water mass fraction.

The liquid flux was measured by observation of the liquid level in the permeate collector at regular intervals, after the system



reached steady state. Data points were immediately plotted and ample measurements were made to insure that a single steady flux was attained for each experimental run.

## CHAPTER V

### SIMULATION OF MEMBRANE-AIDED DISTILLATION

This section describes a simulation of a ten million gallon per year ethanol dehydration plant which would use the membrane-aided distillation process suggested by Gooding and Bahouth (11). This process is depicted in Figure 13 with major design specifications. A computer program was written in Fortran to incorporate the flux and selectivity models developed from experiments with the UOP-TFC801 membrane into the plant subunit calculations. Guthrie's cost correlations (14) were used to determine the installed costs of process units. Simple optimization schemes were applied to several of the design parameters to minimize the total annual cost and to identify important economic trends.

The simulation program was written to iterate four independent variables ( $X_{FDP}$ ,  $X_{D1}$ ,  $X_{D2}$ , and the ratio  $F_{DP}:P$ ) in order to find the optimum plant parameters. Salient points of the simulation program are described in the following paragraphs. Figures 14 and 15 flow-chart the method of calculation. The complete documented computer program listing is displayed in Appendix D.

#### Plant Mass Balance Calculations

It was desired to simulate a plant that would produce ten million gallons of 99.5 mole percent ethanol per year from a 4.2 mole percent (10 mass percent) aqueous ethanol feed stream. Description of the set of mass balance calculations follows. All compositions are expressed in mole fraction of ethanol.



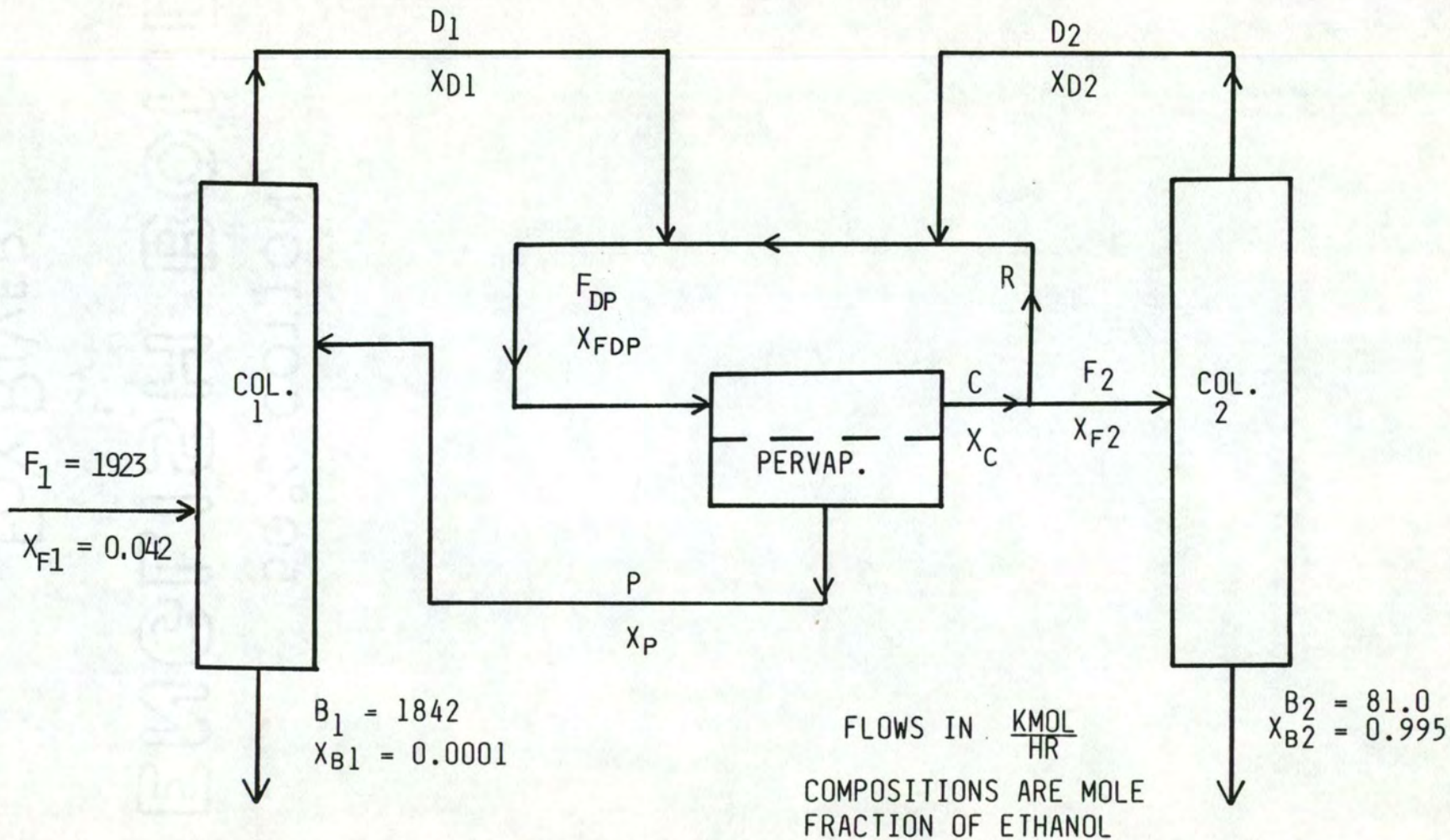


Figure 13. Schematic Diagram of the Membrane-Aided Distillation Process with Overall Mass Balance Parameters

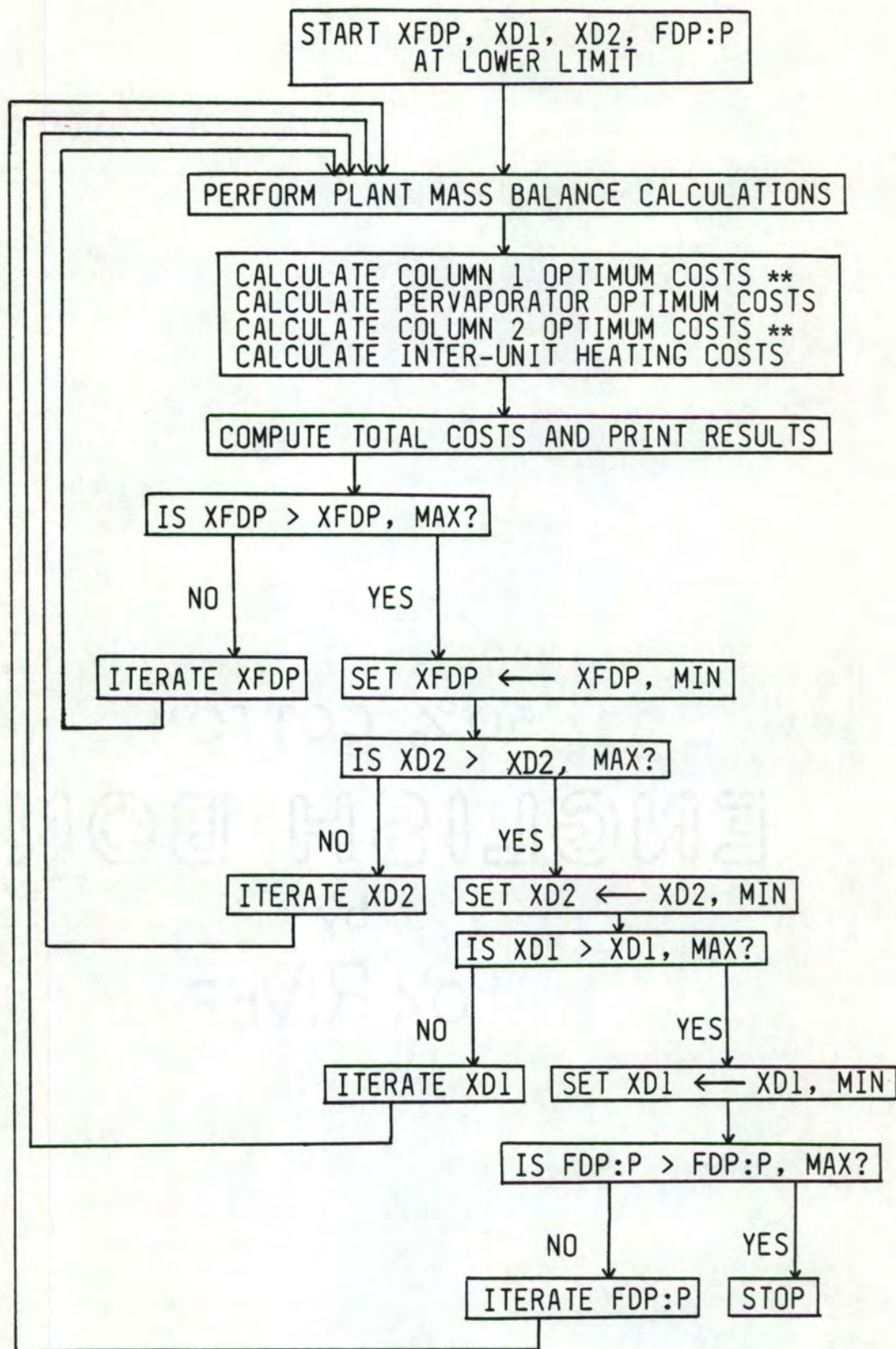


Figure 14. Flow Chart for Simulation Program  
 (\*\* Figure 15 shows a more detailed flow chart for distillation column calculations)



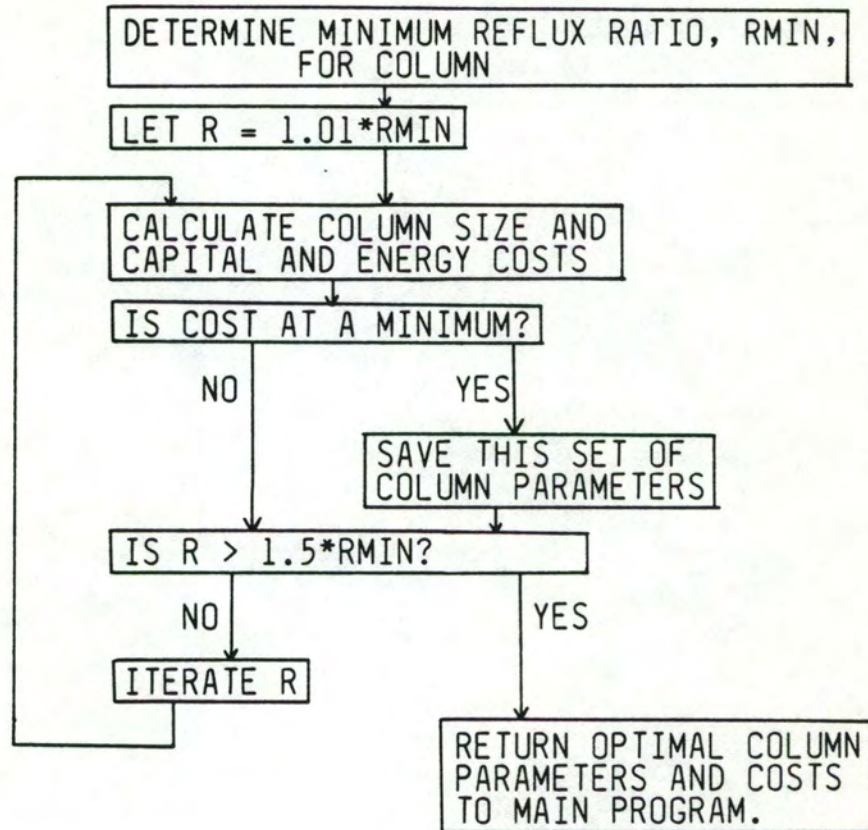


Figure 15. Column Subroutine Flowchart

Overall plant balance. The variables  $X_{F1}$ ,  $X_{B2}$ , and  $B_2$  have been specified for the aforementioned feed quality and product rate and quality. In order to limit product losses in the water waste stream to about 1/4 percent of the product, the mole fraction of ethanol in stream  $B_1$  was chosen as  $X_{B1} = 0.0001$ . With the four values,  $X_{F1}$ ,  $X_{B1}$ ,  $X_{B2}$ , and  $B_2$ , specified, an overall plant mass balance yields values for the column 1 feed and bottoms flow ( $F_1$ ,  $B_1$ ).

Pervaporator section. Next, calculations were performed around the pervaporator section. The membrane selectivity model and mass balances on the pervaporator were used to calculate permeate and concentrate mole fractions ( $X_p$ ,  $X_c$ ). Energy for the phase change that occurs in pervaporation must be extracted from the feed-concentrate stream, and reducing the feed temperature reduces flux. Since the experimental flux data spanned a relatively narrow temperature range, an upper limit for the temperature drop of the feed-concentrate stream was arbitrarily chosen to be 13°C. The temperature drop was accounted for by using an average temperature in the feed stream as the simulation feed temperature. The following three constraints limited the range of operation for this plant design.

1. An energy balance showed that for a temperature drop through the membrane unit to be less than 13°C, the pervaporator feed to permeate ratio must be at least 25:1 ( $F_{DP}:P > 25$ ).
2. The feed mole fraction,  $X_{FDP}$ , must be such that the membrane selectivity model yields a permeate mole fraction that is smaller than the column 1 overhead mole fraction ( $X_p < X_{D1}$ ).
3. The feed mole fraction,  $X_{FDP}$ , also must be such that the column 2 feed mole fraction (which is the same as the concentrate stream mole fraction, i.e.,  $X_{F2} = X_c$ ) is greater than the column 2 overhead mole fraction ( $X_{F2} > X_{D2}$ ).



Items 2 and 3 are both constraints on the value of  $X_{FDP}$  and together they define upper and lower limits of the value of  $X_{FDP}$ . For a particular set of values of  $X_{D1}$ ,  $X_{D2}$ , and the ratio  $F_{DP}:P$ , a particular range of values of  $X_{FDP}$  can be explored.

Column 2. The bottoms (product) stream has been fully specified ( $B_2, X_{B2}$ ). Constraints are that the overhead mole fraction must be greater than that of the azeotrope and less than that of the feed ( $0.894 < X_{D2} < X_{F2}$ ). Then for a particular overhead composition ( $X_{D2}$ ) and a particular feed composition ( $X_{F2}$ ) as calculated from the pervaporator section, a mass balance over column 2 yields feed and overhead flow rates ( $F_2, D_2$ ).

Column 1. The feed and bottoms streams have been specified in the overall plant mass balance ( $F_1, X_{F1}, B_1, X_{B1}$ ). Here the overhead mole fraction must be less than that of the azeotrope and greater than that of the permeate ( $X_p < X_{D1} < 0.894$ ). Then for a particular overhead composition ( $X_{D1}$ ) and a particular permeate composition ( $X_p$ ) as calculated from the pervaporator section, a mass balance over column 1 yields permeate and overhead stream flow rates ( $P, D_1$ ).

Pervaporator section again. With the permeate stream flow rate ( $P$ ) given explicitly by column 1 calculations, the pervaporator feed and concentrate streams ( $F_{DP}, C$ ) may be calculated by a mass balance over the pervaporator.

Recycle loop. A balance around the concentrate stream divider yields a value for the recycle flow ( $R$ ). A balance around the stream mixing sections (with inputs  $D_1, D_2, R$ , and output  $F_{DP}$ ) should yield the previously calculated value of  $F_{DP}$  and the original value of  $X_{FDP}$ .



Summary. In order to perform a complete set of plant mass balances, four variables (in addition to the originally specified variables) must be chosen and their respective constraints adhered to. These are listed in Table II. The simulation program was written to be as general as possible. Therefore each of the chosen variables listed in Table II was iterated between reasonable limits and a complete plant mass balance computation was performed for each set of chosen variables.

#### Plant Subunit Size and Cost Calculations

For each set of plant parameters computed in the mass balance section, size and cost calculations were performed for each subunit. In most cases, installed costs were computed by use of Guthrie's cost correlations (14) corrected to 1984 dollars. These costs were annualized over six years, with the exception of the membrane unit cost which was annualized over three years. Utility costs were computed on an annual basis so that the total annual cost for each plant subunit was calculated.

Columns. Simulation of the distillation columns was done by simple stage-to-stage calculations as in the McCabe-Thiele method. The advantage to using this method was that the vapor-liquid equilibrium data could be precisely modeled over the entire range of operation by use of simple curve-fitting over discrete sections of the equilibrium curve. Constant molal overflow and constant (atmospheric) pressure were assumed. Feed qualities were saturated liquid. A total condenser and partial reboiler were used for each column.



TABLE II. Simulation Chosen Variables and Constraints

Chosen Variable	Constraints
$X_{FDP}$	Must yield $X_{F2} > X_{D2}$ , $X_P < X_{D1}$
$X_{D1}$	$X_P < X_{D1} < X_{AZEO}$ ( $X_{AZEO} = 0.894$ )
$X_{D2}$	$X_{AZEO} < X_{D2} < X_{F2}$
FDP:P ratio	FDP:P > 25

To find the optimum column specifications for given input and output stream specifications, the reflux ratio was varied from near the minimum to about 1.5 times the minimum. The reflux ratio associated with the lowest total annual cost was deemed the optimum.

Pervaporation section. The pervaporation section includes the membrane modules, a condenser, a refrigeration unit and a vacuum pump. The membrane flux model was used to determine the membrane area needed. The cost of the vacuum pump used to vent noncondensables was disregarded. Installed cost calculations were performed for the condenser using Guthrie's correlations(14), and annualized over six years. Installed cost of the membrane unit was estimated to be twice the purchased cost of \$6/ft<sup>2</sup> (36) and annualized over only three years. Installed costs of the refrigeration unit were calculated by use of the correlation appearing in the Chemical Engineers' Handbook (32, Fig. 25-5) and corrected to 1984 dollars. Energy costs for refrigeration were calculated using data from Peters and Timmerhaus (33, p. 881) and corrected to 1984 dollars.

Interunit heat exchange. Analysis of interunit heating requirements indicated the following. A column 1 feed and bottoms exchanger would take care of heating the raw feed to saturation while sufficiently cooling the waste water. Other streams could be provided with necessary sensible heat almost entirely by the column overhead condensers. Total annual costs for interunit heat exchangers were calculated at three conditions, averaged, and thereafter treated as constant. The smoothing effect of annualizing capital costs allowed this to be sufficiently accurate for this simulation.



Total costs. It was desired to express the economics in terms of cost per gallon to upgrade 82.5 mole percent ethanol to 99.5 mole percent ethanol. Therefore a simulation was run for producing 82.5 mole percent ethanol and the cost associated with producing 82.5 mole percent ethanol in column 1 was subtracted from the cost of producing 99.5 mole percent ethanol. This difference was the net cost of upgrading.

## CHAPTER VI

### SIMULATION RESULTS AND DISCUSSION

The purpose of the membrane-aided distillation simulation was to examine the economic feasibility of producing anhydrous ethanol by this method. The question to be answered was whether there is a possible economic advantage of membrane-aided distillation over the conventional azeotropic distillation method in use today. This chapter presents the results of the membrane-aided distillation simulations using the models developed in this study for the UOP-TFC801 membrane. The cost per gallon of producing anhydrous ethanol by this method was compared to the cost per gallon using azeotropic distillation with benzene as the entrainer. For comparison, simulations were also run using the data obtained from the literature for a cellulose 2.5 acetate membrane (28) which was reported to have a higher selectivity and a lower permeation rate.

#### Simulation with the UOP-TFC801 Membrane

Selected stream flows and capital and energy costs for the two columns and the pervaporation section of the membrane-aided distillation plant were plotted against the pervaporator feed stream composition ( $X_{FDP}$ ) with the other independent variables held constant. Figures 16 and 17 present these data. A summary of total costs as a function of pervaporator feed-to-permeate ratio ( $F_{DP}:P$ ), pervaporator feed composition ( $X_{FDP}$ ), and column 2 overhead composition ( $X_{D2}$ ) is presented in Figure 18. It can be seen that the lower ratio of



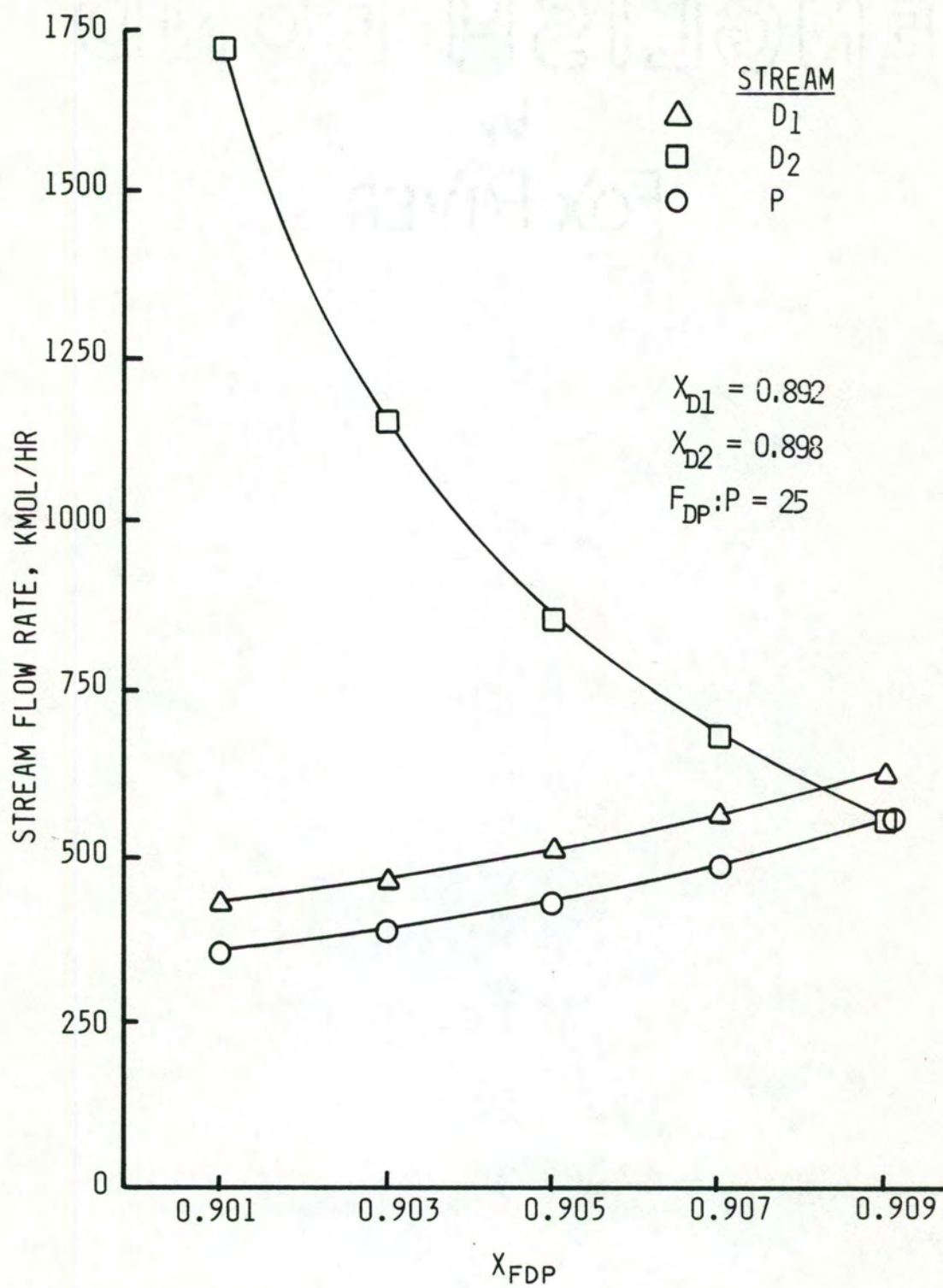


Figure 16. Selected Stream Flows as a Function of  $X_{FDP}$

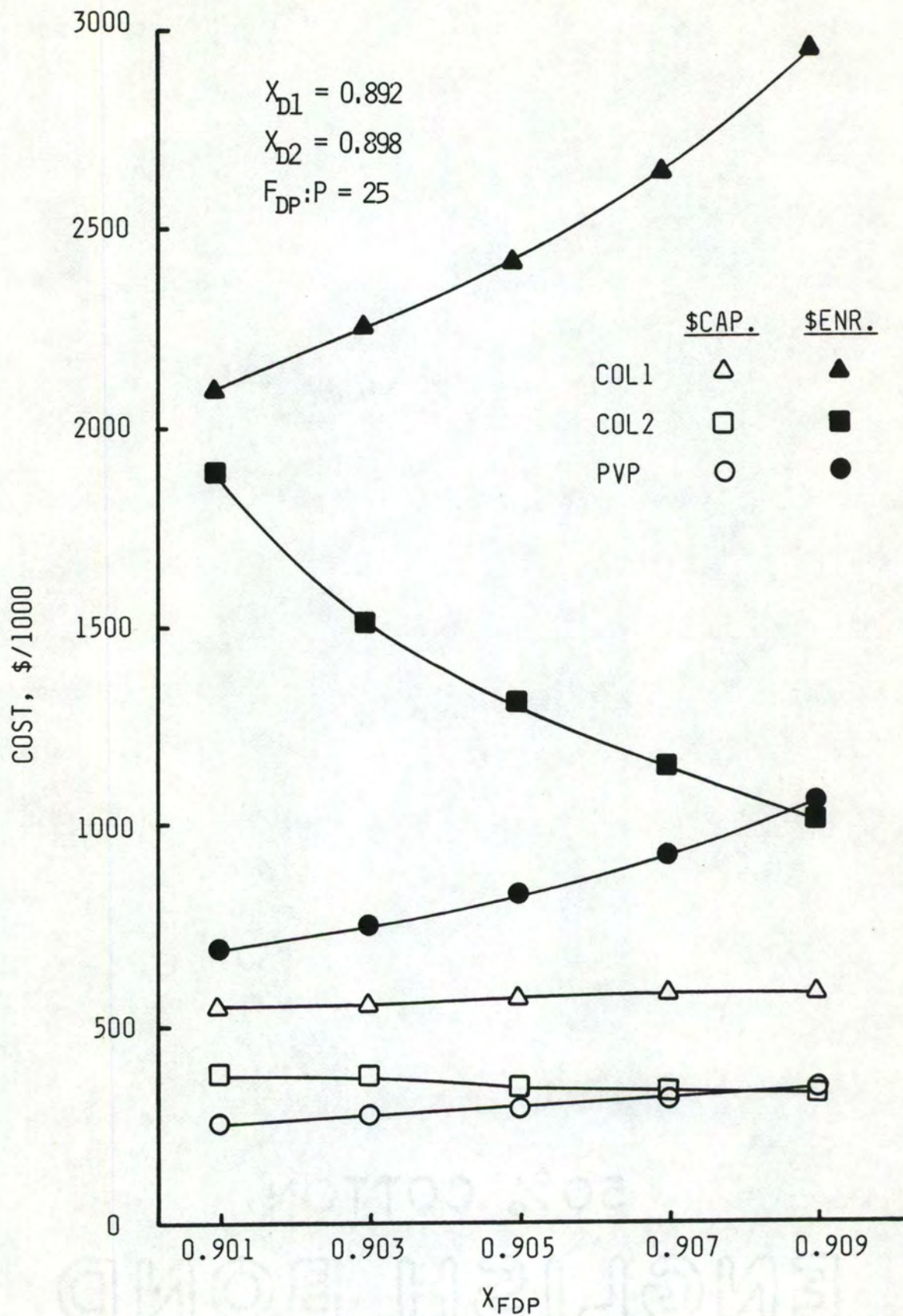


Figure 17. Capital and Energy Costs as a Function of  $X_{FDP}$



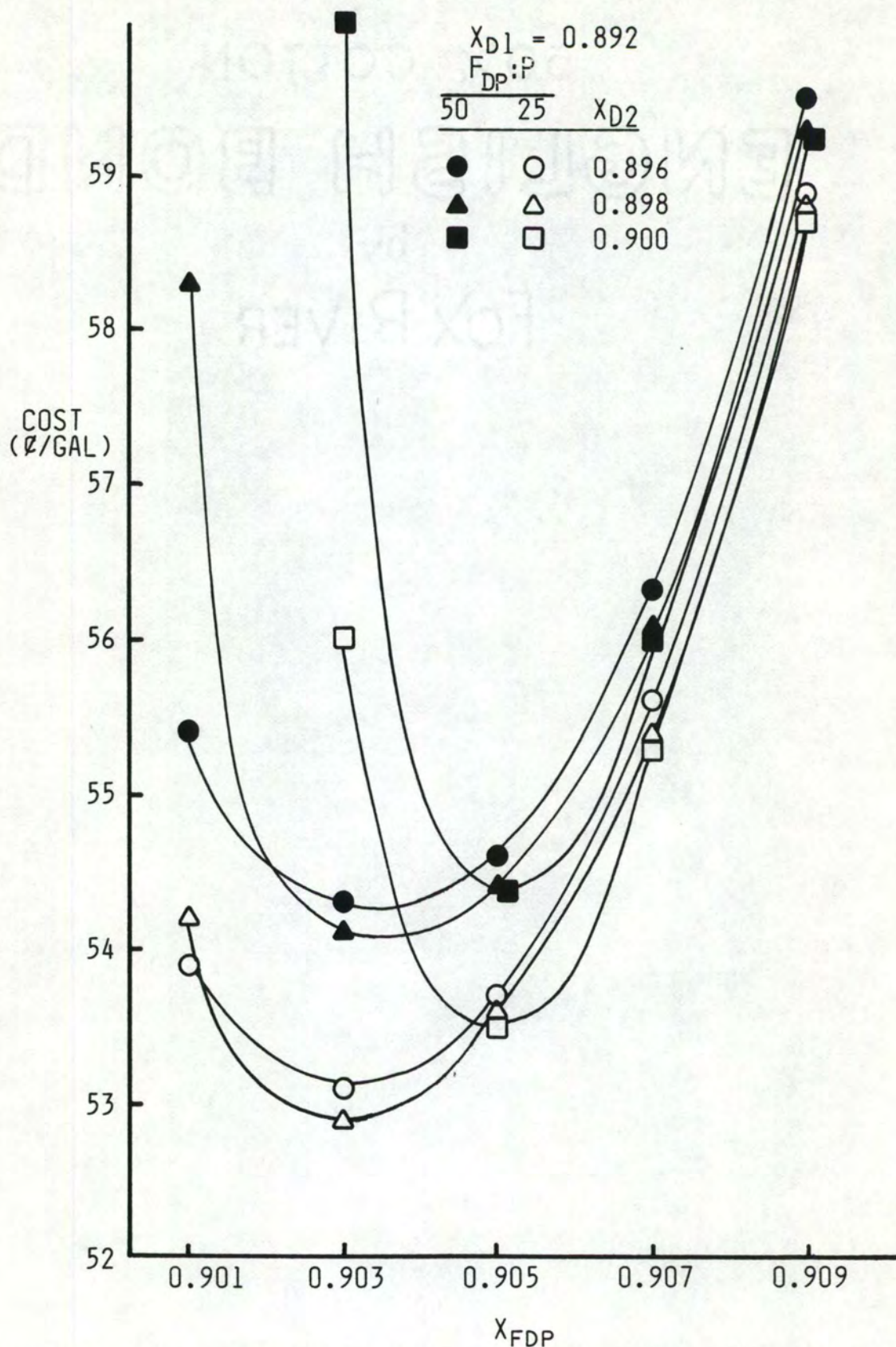


Figure 18. Total Upgrading Costs as a Function of  $X_{FDP}$  with  $X_{D2}$ ,  $F_{DP}:P$  as Parameters



pervaporator feed to permeate ( $F_{DP}:P = 25$ ) yields a lower cost in this case and this is a characteristic trend. Figure 19 then shows total plant cost trends with fixed  $F_{DP}:P = 25$  and independent variables  $X_{FDP}$ ,  $X_{D2}$ , and  $X_{D1}$ .

Stream flows. For specific overhead compositions and pervaporator feed to permeate ratio, the plant mass balance was shown to vary most strongly with changes in the pervaporator feed stream composition,  $X_{FDP}$ . For  $X_{FDP}$  near its lower limit, the overhead of column 2 becomes very large while the pervaporator effluent (stream P) and thus the column 1 overhead streams are at a minimum. For  $X_{FDP}$  near its upper limit, the opposite effect is reflected in the plant mass balance. The overhead of column 2 reaches a minimum and the pervaporator effluent and column 1 overhead streams reach a maximum. This shift between permeate and column 1 overhead streams on the one hand and the column 2 overhead stream on the other indicates that an optimum pervaporator feed composition,  $X_{FDP}$ , may be found.

Capital and energy costs. Capital and energy costs for each processing unit are represented in Figure 17 as a function of pervaporator feed composition ( $X_{FDP}$ ) with pervaporator feed-to-permeate ratio and column overhead compositions held constant ( $F_{DP}:P = 25$ ,  $X_{D1} = 0.892$ ,  $X_{D2} = 0.898$ ). Comparing Figure 17 to Figure 16, one can observe that increased stream flows most pronouncedly increase energy costs with relatively small influence on capital costs. The total annual cost of these units is shown to be at a minimum for pervaporator feed composition at about  $X_{FDP} = 0.903$ .



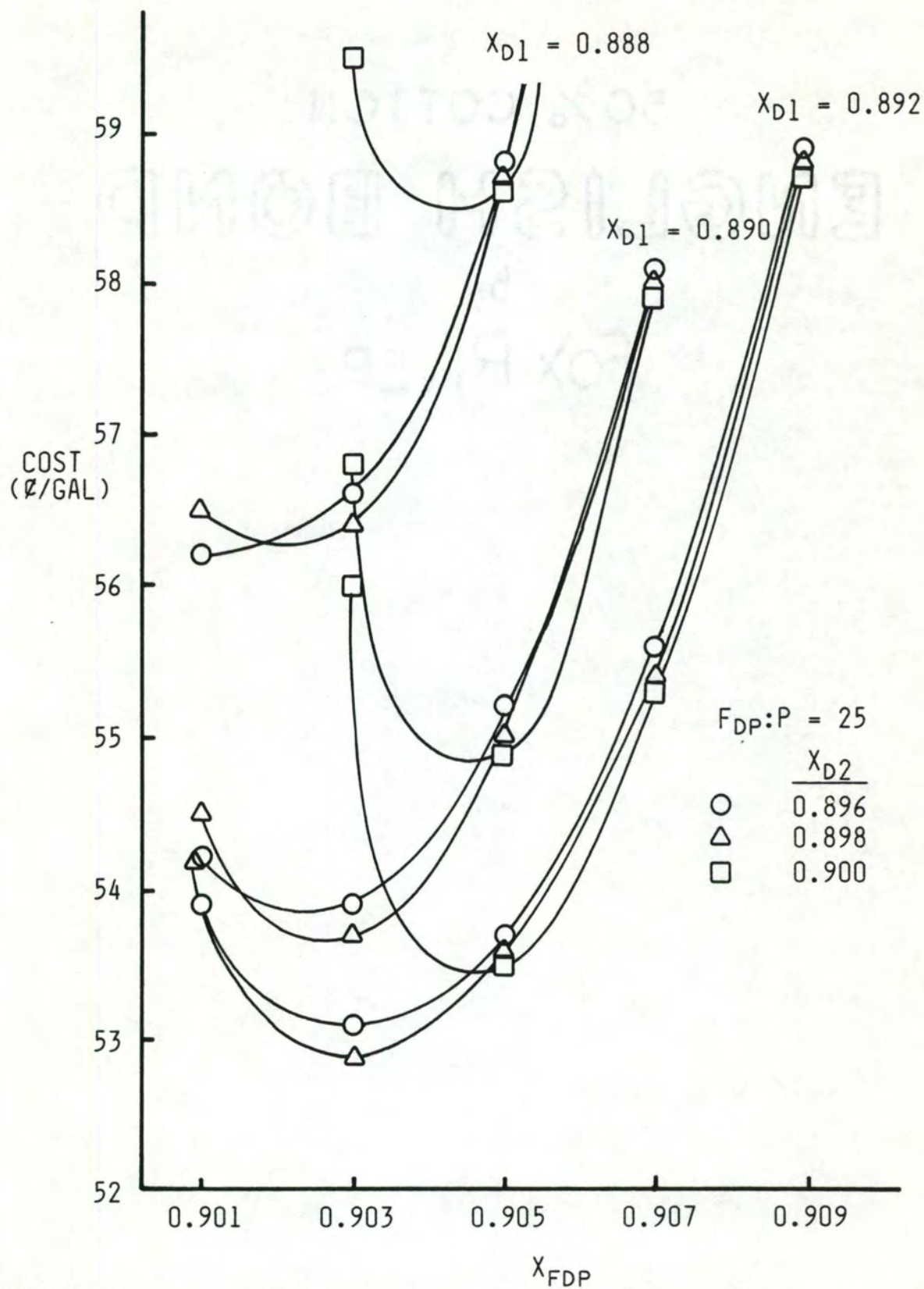


Figure 19. Total Upgrading Costs as a Function of  $X_{FDP}$  with  $X_{D1}$ ,  $X_{D2}$  as Parameters



Pervaporator feed stream to permeate stream flow ratio. With the assumption of isothermal operation at an average feed-concentrate temperature simulations showed that reducing the pervaporator feed to permeate flow ratio ( $F_{DP}:P$ ) reduced annual cost. The plant mass balance dictated that a higher pervaporator feed flow ( $F_{DP}$ ) at a specified composition ( $X_{FDP}$ ) meant that a higher load would be put on column 2. This is because the column 2 overhead stream is mainly responsible for enriching the recycle stream back to its specified composition,  $X_{FDP}$ . Thus the energy costs of column 2 rose most prominently for the case of increased  $F_{DP}:P$  ratio as illustrated in Table III.

#### Inaccuracy in the Simulation

The major potential sources of inaccuracy are probably the vapor-liquid equilibrium data and the approximate nature of the cost correlations. Vapor-liquid equilibrium data above 89.4 mole percent ethanol were sparse and often inconsistent. These data were necessary for size and cost calculations of column 2. Data from six experimenters were plotted and a composite curve was modeled and used for vapor-liquid equilibrium calculations in this range. This curve appears in Appendix E.

Another major limit to accuracy is due to the approximate nature of the cost correlations. However, these correlations are sufficient to show the cost trends and to provide a preliminary indicator of cost feasibility of the process.

Other sources of inaccuracy due to simplifying assumptions were relatively minor. Appendix D contains a detailed, documented computer



TABLE III. Capital and Energy Costs as a Function of Pervaporator Feed to Permeate Ratio

---

For  $X_{D1} = 0.892$   
 $X_{D2} = 0.898$   
 $X_{FDP} = 0.903$

$F_{DP}:P$	ENERGY COST (thousand \$)			CAPITAL COST (thousand \$)		
	COL1	PVP	COL2	COL1	PVP	COL2
25	2250	750	1512	545	271	371
50	2250	764	1602	545	269	382

---



listing of the simulation program complete with simplifying assumptions where applicable.

Cost comparison. The cost incentive for producing anhydrous ethanol from 82.5 mole percent is obscured by various government programs that promote the production of fuels from biomass. The cost of dehydration using azeotropic distillation is reportedly about 25 cents per gallon of anhydrous product (22). The minimum upgrading cost from the membrane-aided distillation simulations was found to approach 53 cents per gallon for the conditions studied, as shown in Figure 19.

#### Simulation Using a More Selective Membrane

The UOP-TFC801 membrane is an example of a very high flux and low selectivity membrane, with fluxes on the order of  $0.25 \text{ kmol}/(\text{m}^2\text{-hr})$  and a separation factor of 1.4. To begin to explore the trade-off in plant economics between a high flux and low selectivity membrane on the one hand and a lower flux but higher selectivity membrane on the other, simulations were performed using literature data on a more selective ( $\alpha = 11$ ), lower flux (flux =  $0.016 \text{ kmol}/(\text{m}^2\text{-hr})$ ) cellulose 2.5 acetate membrane (28). Data for this membrane were available at only one set of conditions (see Table I). Therefore, the previously independent variable,  $X_{FDP}$ , was specified as constant, leaving  $X_{D1}$ ,  $X_{D2}$ , and  $F_{DP:P}$  as the independent variables. The results of these simulations appear in Figure 20 and indicate that plant costs could be as little as 13 cents per gallon of anhydrous ethanol produced if the cost of the membrane were the same as the UOP-TFC801. This is well below the current estimated cost of 25 cents per gallon using azeotropic distillation.



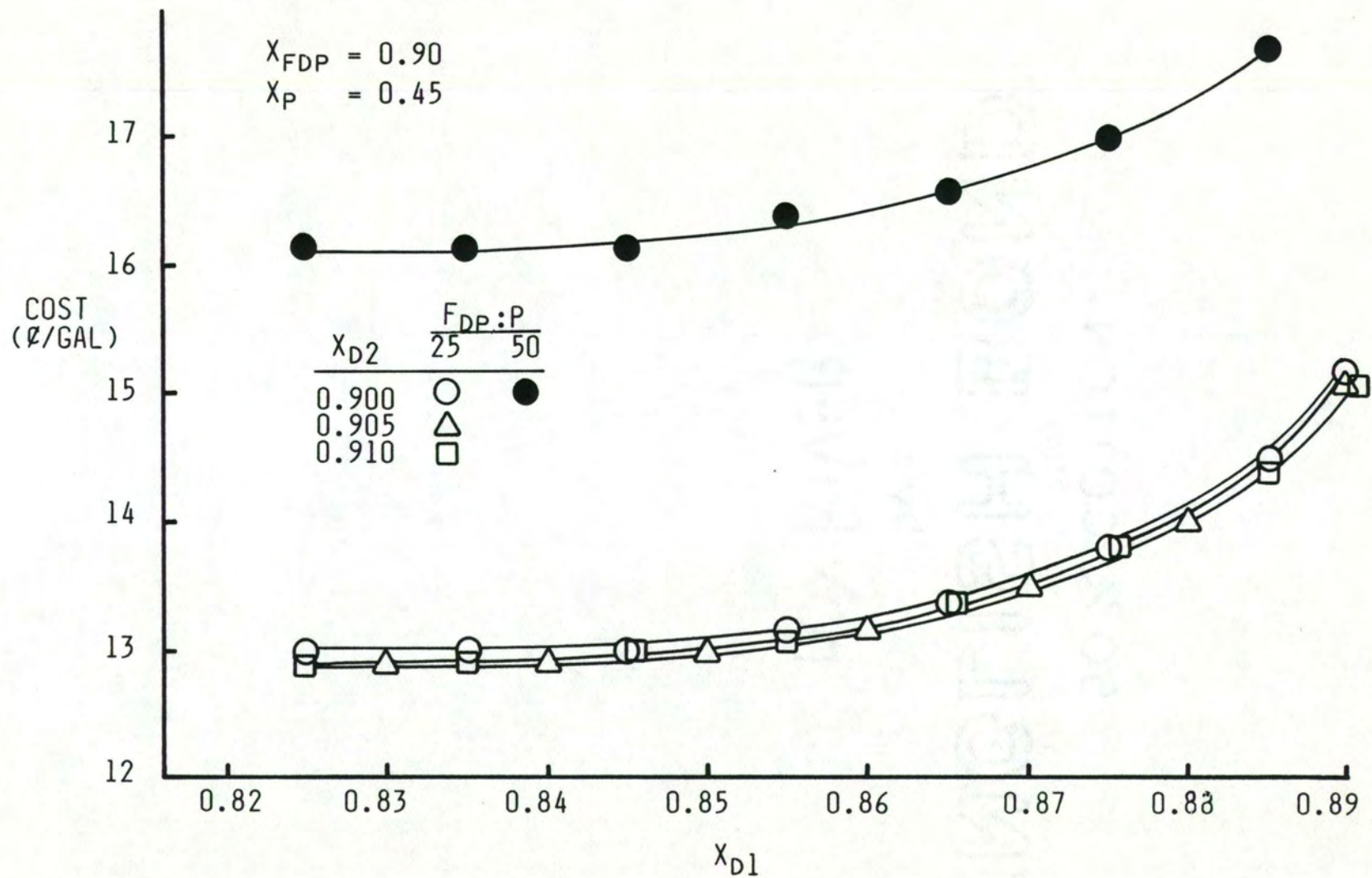


Figure 20. Total Upgrading Costs Using a More Selective Membrane

Referring to Figure 20, it is significant that the feed to permeate ratio,  $F_{DP}:P$  has a relatively large effect on the total cost for this more selective membrane. This ratio was constrained to be above 25 in the calculations, which corresponds to a temperature drop through the membrane unit of about  $13^{\circ}\text{C}$ . If the temperature drop constraint of  $13^{\circ}\text{C}$  across the membrane unit were relaxed, an even lower upgrading cost may be obtainable. This possibility was not explored in this study because flux versus temperature data were not available to support the calculations.



## CHAPTER VII

### CONCLUSIONS

Based on the pervaporation experiments and membrane-aided distillation simulations, the following conclusions may be drawn:

1. Pervaporation of azeotropic ethanol/water mixtures through the UOP-TFC801 membrane yielded fluxes on the order of 0.25 kmol/(m<sup>2</sup>-hr) with a separation factor of 1.4. Flux was found to increase at increased feed temperatures and at decreased permeate pressures. Selectivity was found to be a function of feed composition only.
2. The lowest costs associated with upgrading 82.5 mole percent ethanol to anhydrous ethanol using the UOP-TFC801 membrane in a membrane-aided distillation scheme were found to be about 53¢/gal of anhydrous ethanol produced. This is roughly double the cost of upgrading using conventional azeotropic distillation, indicating that membrane-aided distillation using this high flux, low selectivity UOP-TFC801 membrane is not economically attractive.
3. Simulation of the membrane-aided distillation process using models for a membrane with lower flux but higher selectivity indicated a cost on the order of 13¢/gal product, or about one half the cost of azeotropic distillation. The implication is that membrane-aided distillation looks attractive for production of anhydrous ethanol with membranes which are more selective.



## CHAPTER VIII

### RECOMMENDATIONS

Based on the results of this study, the following recommendations are proposed.

1. In the laboratory, install a cold trap in the vacuum line between the condenser and the vacuum pump in order to minimize permeate vapor losses, or develop a smaller-scale system that uses cold traps exclusively.
2. Obtain membranes which are reported to have a higher selectivity than the UOP-TFC801 and moderate fluxes. Test these membranes in the laboratory on the ethanol/water system and obtain models for operation over a wide range of conditions. Simulate the membrane-aided distillation plant using these models and re-evaluate the scheme.
3. Use the simulation program and assumed membrane performance to evaluate membrane-aided distillation for the separation of other azeotrope-forming solutions in which the relative volatility is a stronger function of composition and the azeotropic composition is not as close to one pure component as it is with ethanol/water. For example, it may be economically attractive to separate isopropanol/water with a high flux, low selectivity membrane such as the UOP-TFC801. If the simulation indicates feasibility, conduct laboratory experiments to refine the pervaporation model.
4. Explore ways to improve the pervaporation section of the membrane-aided distillation plant which would minimize refrigeration costs and product losses. These might include use of in-line compressors and heat exchangers to recover the latent heat of vaporization from the permeate stream. See refs. (11,23) for more detail on this concept.
5. Explore further the optimization of the membrane-aided distillation plant by using a non-isothermal membrane unit model and allowing a wider range of feed-concentrate temperature drops in the simulations.
6. Upgrade the simulation program to include more detailed and more precise cost correlations. For example, a subroutine could be written to simulate inter-unit heat exchange costs for each set of plant parameters.



NOT TO BE

ENGLISH BOARD

APPENDICES

## Appendix A

## Pervaporation Laboratory Data and Results

Tables A-I and A-II present pervaporation data from the laboratory along with calculated fluxes and separation factors. Table A-I presents data for experiments in which the feed composition was held constant while the feed temperature and permeate pressure were varied. Table A-II presents data for experiments in which the feed composition was varied while the feed temperature and permeate pressure were held constant.

The data given are temperature of the feed ( $T_1$ ), permeate pressure ( $P_2$ ), rate of liquid level rise in the collector ( $dz/dt$ ), purge stream rotameter measurement ( $V$ ), mass fraction of water in the feed ( $X_F$ ), mass fraction of water in the permeate liquid ( $X_P$ ), ethanol flux ( $G_A$ ), water flux ( $G_W$ ), total flux ( $G_{TOT}$ ), separation factor ( $S$ ).



TABLE A-1. Laboratory Data and Calculated Results for Constant Feed Composition Experiments

Run No.	T <sub>1</sub> (°C)	P <sub>2</sub> (mmHg)	dz/dt (in/min)	V (sccm)*	X <sub>F</sub>	X <sub>P</sub>	G <sub>A</sub> $\left(\frac{\text{kmol}}{\text{m}^2\text{-hr}}\right)$	G <sub>W</sub> $\left(\frac{\text{kmol}}{\text{m}^2\text{-hr}}\right)$	G <sub>TOT</sub> $\left(\frac{\text{kmol}}{\text{m}^2\text{-hr}}\right)$	S
2	37.5	30.	0.0496	100	5.05	9.96	0.1849	0.0488	0.2337	1.94
3	37.5	50.	0.0396	72	4.95	6.40	0.1369	0.0235	0.1605	1.29
4	37.5	70.	0.0322	52	4.98	6.12	0.1047	0.0173	0.1219	1.23
9	42.5	30.	0.0568	120	4.95	7.16	0.2279	0.0431	0.2710	1.42
10	42.5	50.	0.0593	60	4.93	7.75	0.1838	0.0388	0.2226	1.59
11	42.5	70.	0.0506	52	4.82	6.12	0.1562	0.0259	0.1821	1.28
5	47.5	30.	0.0813	94	4.97	6.93	0.2741	0.0511	0.3252	1.39
6	47.5	50.	0.076	68	4.98	6.70	0.2360	0.0429	0.2789	1.35
8	47.5	50.	0.0675	80	4.90	6.71	0.2189	0.0396	0.2585	1.37
7	47.5	70.	0.0710	54	4.89	7.33	0.2120	0.0424	0.2544	1.52

\* standard cubic centimeters per minute



TABLE A-II. Laboratory Data and Calculated Results for Constant Feed Temperature and Permeate Pressure Experiments

Run No.	T <sub>1</sub> (°C)	P <sub>2</sub> (mmHg)	dz/dt (in/min)	V (sccm)*	X <sub>F</sub>	X <sub>P</sub>	G <sub>A</sub> $\left(\frac{\text{kmol}}{\text{m}^2\text{-hr}}\right)$	G <sub>W</sub> $\left(\frac{\text{kmol}}{\text{m}^2\text{-hr}}\right)$	G <sub>TOT</sub> $\left(\frac{\text{kmol}}{\text{m}^2\text{-hr}}\right)$	S
12	42.5	30.	0.0688	100	0.21	0.25	0.2603	0.0019	0.2622	1.33
13	42.5	30.	0.0717	115	0.28	0.82	0.2817	0.0066	0.2883	3.26
14	42.5	30.	0.0710	105	0.95	1.27	0.2685	0.0096	0.2781	1.46
15	42.5	30.	0.0715	103	1.74	2.74	0.2642	0.0202	0.2844	1.69
16	42.5	30.	0.0646	113	2.46	3.73	0.2514	0.0261	0.2775	1.61
17	42.5	30.	0.0677	100	3.35	5.0	0.2456	0.0332	0.2788	1.52
18	42.5	30.	0.0653	115	4.30	5.86	0.2502	0.0392	0.2894	1.36
19	42.5	30.	0.0633	110	5.06	6.70	0.2380	0.0424	0.2804	1.31
20	42.5	30.	0.0623	100	6.14	8.37	0.2229	0.0498	0.2726	1.34
21	42.5	30.	0.0578	110	11.40	13.52	0.2076	0.0758	0.2834	1.11
22	42.5	30.	0.0502	105	28.32	25.02	0.1643	0.1194	0.2837	0.72
23	42.5	30.	0.0425	115	53.81	35.08	0.1376	0.1475	0.2851	0.36
24	42.5	30.	0.0313	120	73.19	45.5	0.1039	0.1493	0.2531	0.21

\* standard cubic centimeters per minute



## Appendix B

### Materials and Apparatus

Appendix B is divided into two sections. The first section presents descriptions of materials used in the pervaporation laboratory. The second section presents descriptions of materials used in the titration laboratory.

#### Pervaporation Laboratory Materials and Apparatus

Condenser. The condenser was used to condense the permeating vapors for collection in the attached collector. The refrigerant flowed in the tube side while the permeate occupied the shell side. It was a Ross Model SSCF heat exchanger, constructed of stainless steel, with 56 tubes that provided 4.3 square feet of heat transfer surface area.

Ethanol. The ethanol used in the pervaporation experiments was anhydrous 200 pf Ethyl Alcohol U. S. P., produced by Aaper Alcohol and Chemical Co. (DSP KY 417) Shelbyville, KY. It was obtained from the Clemson University dispensary.

Feed heat exchanger. A small (approximately one square foot of heat transfer surface area) heat exchanger was used to maintain the feed temperature. Low pressure steam on the shell side was used for heating.

Feed pump. The feed pump was a 1/3 hp, 3450 rpm centrifugal pump. It was an Eastern Model F-34B Type 107.

Feed side pressure gauge. The feed side pressure gauge was an Ashcroft, Duragauge with a measurement range of 0 to 60 psig.

Feed tank. A 15 liter stainless steel tank was used as the feed tank.

Flow meter, liquid. The feed flow rate to the membrane module was measured with a Brooks Instrument Co. Type 9-1110-10 rotameter, calibrated for flows of 0 to 4.4 gpm of water.

Flow meter, vapor. The purge stream flow rate was measured with a Brooks Instrument Co. Type I-1355 rotameter with tube type 2-15-3 using a 1/8 inch diameter stainless steel ball float, calibrated for an air flow of 15 to 200 sccm at 30 mmHg abs and 40 °F.

Manometer. The permeate pressure was measured by an absolute mercury manometer. It was a Meriam Instrument Co. Model 11AA10WM and had 1 mm gradations.

Membrane. A commercial reverse osmosis sea water membrane, the UOP-TFC801, manufactured by UOP, Inc., Fluid Systems Div., San Diego, CA, was used for the pervaporation experiments. It was constructed of a thin film composite of polyamide on polysulfone.

Membrane module. The body of the membrane module was constructed of two 3-inch-to-1-inch Pyrex Double Tough glass pipe adapters. The membrane was held between the 3-inch openings. A 1/32 inch thick perforated stainless steel plate was used as a membrane support. A smooth bead of epoxy was laid on the perimeter of the support plate to provide a solid surface for sealing. Figure B-1 illustrates the sealing



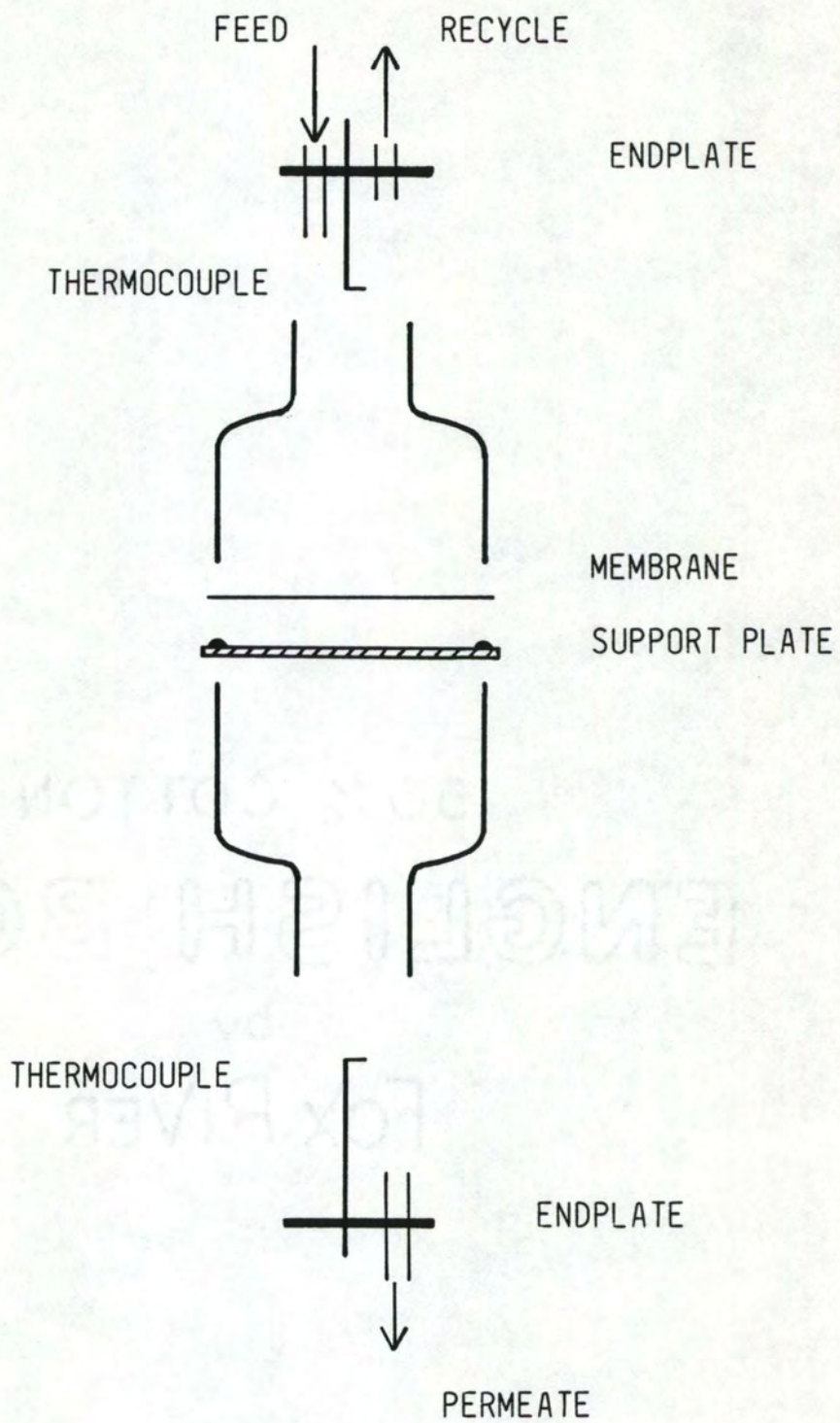


Figure B-1. Diagram of Pervaporation Module

arrangement. Stainless steel endpieces were attached to the open ends of the glass pipe fittings which provided the inlet and outlet piping attachments along with thermocouple attachments. The fittings and endpieces were held together by standard aluminum (glass pipe) clamps.

Permeate collector. A vertically held one inch i.d. Pyrex tube was used to collect the permeate liquid flowing from the condenser. An attached scale allowed for determination of relative height of liquid in the collector.

Piping. All piping on the feed side was constructed of 1/4 inch 316 stainless steel pipe or 1/4 inch 316 stainless steel tubing. The purge stream utilized Tygon heavy-walled vacuum tubing. The refrigeration section used plastic tubing.

Refrigerant. A 50-50 mixture of ethanol/water was used as the cooling liquid in the condenser.

Refrigerant pump. The refrigerant pump was a 1/5 hp, 6000 rpm centrifugal pump. It was an Eastern Model E7, Type 102.

Refrigeration unit. A water cooled Dunham-Bush Heat-X CCP Cast Cooler Package, Model CCP25W was used to cool the refrigerant for the permeate condenser.

Thermocouples. The thermocouples were made of copper-constantan wire, twisted and soldered.

Temperature readout. The temperature readout was an Analog Devices Model AD2036 with ports for 6 thermocouples. It was calibrated to within 0.2 °C in the 0 to 50 °C range.



Vacuum pump. The low permeate pressure was maintained by use of a vacuum pump which also purged the system of noncondensables. It was a Welch Scientific Co. Model 1402 oil ring pump.

Water. Distilled water was used to make up the ethanol/water mixtures.

#### Titration Materials and Apparatus

Microbalance. The microbalance was used to measure the mass of liquid samples which were injected into the Fischer titrimeter. It was a Sartorius Type 2433 with a readout to one ten thousandth of a gram.

Karl Fischer reagent. The Karl Fischer reagent was used in the titrations to determine mass percent of water in the injected samples. It is a mixture of iodine, sulfur dioxide, pyridine, and methanol. It was produced by Fisher Scientific Co., Type SO-K-3, and was rated to have a minimum titer of 5.0 mg water per ml.

Solvent. A methanol solvent was used in the titration mixing vessel. It was produced by Fisher Scientific Co., Type A-412, and rated to be 99.9 percent pure.

Titrimeter. The Karl Fischer titrimeter was used for determination of mass percent of water in the ethanol/water samples. It was a Fisher Scientific Co. Model 391 which used an amperometric method of titration to detect the endpoint electrometrically.

Appendix C

Pervaporation Data Reduction Program Listing

SON COTTON  
ENGLISH BOND  
FOX RIVER



C THIS IS A PROGRAM TO CALCULATE TOTAL FLUX THROUGH THE PERVAPORATIVE  
 C MEMBRANE FOR THE BINARY ETHANOL/WATER FEED. VAPOR LOSS ON THE  
 C PERMEATE (VACUUM) SIDE IS ACCOUNTED FOR. THE ASSUMPTIONS PERTAINING  
 C TO THE VAPOR FLOW ARE AS FOLLOWS:  
 C 1) THE VAPOR IS IN EQUILIBRIUM WITH THE LIQUID IN THE COLLECTOR.  
 C 2) THE EQUILIBRIUM TEMPERATURE OF THIS VAPOR IS 10 DEG C.  
 C (THIS TEMP, T5, IS ACTUALLY BETWEEN 8 AND 10 DEG C.)  
 C 3) THE ROTAMETER CORRECTION FROM CALIBRATION CONDITIONS IS THE  
 C SQRT OF THE RATIO OF ACTUAL TO CALIBRATION DENSITIES.  
 C \*\*\*\*\*

C LIST OF VARIABLES

C ALPHA SEPARATION FACTOR  
 C DZDT LIQUID COLLECTION RATE, INCHES HEIGHT/MIN  
 C GA ALCOHOL FLUX, KMOL/(SQM\*HR)  
 C GTOT TOTAL FLUX THROUGH MEMBRANE, KMOL/(SQM\*HR)  
 C GW WATER FLUX, KMOL/(SQM\*HR)  
 C K # LINES OF DATA  
 C MA MOL WT ALCOHOL, 46.07 G/MOL  
 C MAIR MOL WT AIR, 29 G/MOL  
 C MBARL MEAN MOL WT OF LIQUID, G/MOL  
 C MBARV MEAN MOL WT OF VAPOR STREAM, G/MOL  
 C MW MOL WT WATER, 18.016 G/MOL  
 C NA TOTAL FLOW OF ALCOHOL, MOL/HR  
 C NC VAPOR FLOW USING CALIBRATION CONSTANTS (UNCORRECTED), MOL/HR  
 C NL LIQUID MOLAR COLLECTION RATE, MOL/HR  
 C NLA LIQUID ALCOHOL COLLECTION RATE, MOL/HR  
 C NLW LIQUID WATER COLLECTION RATE, MOL/HR  
 C NRUN RUN NUMBER  
 C NV VAPOR MOLAR FLOW RATE (LOSSES) THROUGH VACUUM SIDE, MOL/HR  
 C NW TOTAL FLOW OF WATER, LIQUID AND VAPOR, MOL/HR  
 C PBARS EQUILIBRIUM SATURATED PRESSURE OF A/W VLE SYSTEM, MMHG  
 C P2 PERMEATE PRESSURE, MMHG  
 C QL LIQUID COLLECTION RATE, CC/HR  
 C QS VAPOR FLOW AT CALIBRATION CONDITIONS, CC/HR  
 C RA REJECTION OF ALCOHOL, PERCENT  
 C RHOL DENSITY OF LIQUID PERMEATE, G/CC  
 C T5 TEMPERATURE AT ENTRANCE TO ROTAMETER FOR VAPOR, DEG C  
 C T1 FEED TEMPERATURE, DEG C  
 C V BROOKS ROTAMETER READING,  $0 < V < 15$   
 C XFMASS MASS FRACTION WATER IN FEED TIMES 100 %, PERCENT  
 C XPMASS MASS FRACTION WATER IN PERMEATE TIMES 100 %, PERCENT  
 C XFNW MOLE FRACTION WATER IN FEED, FRACTION  
 C XFNA MOLE FRACTION ALCOHOL IN FEED, FRACTION  
 C XWP WATER MOLE FRACTION IN PERMEATE LIQUID COLLECTED  
 C YABI MOLE FRACTION ALCOHOL IN VAPOR FOR BINARY VLE SYSTEM  
 C YWBI MOLE FRACTION WATER IN VAPOR FOR BINARY VLE SYSTEM  
 C YA VAPOR FRACTION ALCOHOL (TERNARY)  
 C YW VAPOR FRACTION WATER  
 C YAIR VAPOR FRACTION AIR  
 C ZMA DUMMY VARIABLE USED TO CALCULATE MOLE FRACTION  
 C ZMW DUMMY VARIABLE USED TO CALCULATE MOLE FRACTION  
 C ZPA PERMEATE MOLE FRACTION ALCOHOL



```

C ZPW PERMEATE MOLE FRACTION WATER
C*****
C
REAL MBARL, MBARV, NL, NV, NLA, NLW, NC, NW, NA
REAL MA, MW, MAIR
DATA MA, MW, MAIR/46.07, 18.016, 29./
C
C PRINT HEADER
C
PRINT100
100 FORMAT(/, ' RUN#', 2X, ' T1', 5X, ' P2', 4X, ' XWF', 2X, ' -- FLUXA', 3X,
& ' FLUXW --PBARS', 1X, ' XWP', 4X, ' NL', 4X, ' YW', 7X,
& ' NV', 4X, ' GTOT', 3X, ' ZW', 5X, ' ALPHA', /)
PRINT, ('* *', J=1, 28)
C
C READ DATA: K = # LINES OF DATA
C
READ, K
C
DO 11 I = 1, K
READ, NRUN, T1, P2, DZDT, V, XFMASS, XPMASS
C
C CALCULATIONS
C LIQUID COLLECTED, QL(CC/HR)
QL = 772.*DZDT
C
C MOLE FRACTION WATER IN FEED (FROM MASS PERCENT XFMASS)
ZMW = XFMASS
ZMA = 100. - XFMASS
XFNW = ZMW*MA/(ZMW*MA + ZMA*MW)
XFNA = 1. - XFNW
C
C MOLE FRACTION WATER IN PERMEATE (FROM MASS PERCENT XPMASS)
ZMW = XPMASS
ZMA = 100. - XPMASS
XNW = ZMW*MA/(ZMW*MA + ZMA*MW)
XNA = 1. - XNW
C
C MEAN MOL WT OF LIQUID, MBARL(G/MOL)
MBARL = XNW*MW + XNA*MA
C
C DENSITY OF LIQUID PERMEATE, RHOL(G/CC), BASED ON MASS % WATER
CALL CRHOL(XPMASS, RHOL)
C
C LIQUID MOLAR FLOW, NL(MOL/HR)
NL = QL*RHOL/MBARL
NLW = XNW*NL
NLA = XNA*NL
C
C VAPOR LOSS FLOW
C ROTAMETER CALIBRATION TO GET NC(MOL/HR)
CALL CNC(V, NC)
C
C EQUILIBRIUM VAPOR FRACTION ALCOHOL, YABI, BASED ON SATURATED VLE DATA

```



```

      CALL CYABI(XNA, YABI)
C   EQUILIBRIUM SAT VAPOR PRESSURE OF MIXTURE (FROM VLE DATA)
      CALL CPBARS(XNA, PBARS)
C
C   VAPOR FRACTIONS (TERNARY A/W/AIR)
      YA = YABI*PBARS/P2
      YWBI = 1. - YABI
      YW = YWBI*PBARS/P2
      YAIR = 1. - (YA + YW)
C
C   MEAN MOL WT VAPOR, MBARV(G/MOL)
      MBARV = YA*MA + YW*MW + YAIR*MAIR
C
C   VAPOR FLOW, CORRECTED FROM CALIBRATION CONDITIONS--LET T5 = 10 DEG C
      T5 = 10.
      NV = 16.39*NC/SQRT(MBARV)*SQRT(P2/(T5 + 273.16))
C
C   COMPONENT TOTAL FLUXES, GW, GA(KMOL/SQM*HR)
      NW = XNW*NL + YW*NV
      GW = NW/4.56
      NA = XNA*NL + YA*NV
      GA = NA/4.56
C
C   PERMEATE MOLE FRACTIONS
      GTOT = GA + GW
      ZPW = GW/GTOT
      ZPA = GA/GTOT
C
C   MEMBRANE REJECTION OF ALCOHOL, RA = ((CAF - CAP)/CAF)*100 %
      RA = (1. - (1. - ZPW)/(1. - XFNW))*100.
C
C   MEMBRANE SEPARATION FACTOR, ALPHA
      ALPHA = ZPW*(1.0 - XFNW)/(XFNW*(1.0 - ZPW))
C
C   PRINT RESULTS, THEN READ NEXT LINE OF INPUT DATA
      PRINT200, NRUN, T1, P2, XFNW, GA, GW, PBARS, XNW, NL, YW, NV, GTOT, ZPW, ALPHA
200  FORMAT(/, I4, 2X, 2F7.1, 3F9.4, F7.1, 6F8.4, F8.2)
C
11  CONTINUE
      STOP
      END
C -----
C   SUBROUTINES
C
      SUBROUTINE CRHOL(X, RHOL)
      IF(X.LE.60.) THEN
        RHOL = 0.0024*X + 0.798
      ELSE
        RHOL = 0.00144*X + 0.856
      END IF
      RETURN
      END
C ---
C   CURVE FIT TO ROTAMETER, QS(CC/HR), WHERE "V" IS METER READING

```

```

C      0 < V < 15
SUBROUTINE CNC(V, NC)
REAL NC
  QS = 2.88*V**1.73 + 14.5
  NC = 2.48E-3*QS
RETURN
END

C---
C CURVE FIT TO ETHANOL/WATER VLE DATA
SUBROUTINE CYABI(X, Y)
  IF(X.LE.0.3)THEN
    Y = 0.98*X**0.38
  ELSE IF(X.LE.0.7) THEN
    Y = 0.40*X + 0.50
  ELSE IF(X.LE.0.9) THEN
    Y = 0.55*X + 0.395
  ELSE
    Y = 2.129*(X - 0.9)**1.29 + 0.89
  END IF
RETURN
END

C---
C SATURATED VAPOR PRESSURE OF A/W MIXTURE FROM VLE DATA
SUBROUTINE CPBARS(X, P)
  IF(X.LE.0.3) THEN
    P = 22.25*X**0.64 + 0.92
  ELSE IF(X.LE.0.7) THEN
    P = 23.53 + 3.32*ALOG(X)
  ELSE IF (X.LE.0.9) THEN
    P = 8.*X + 16.7
  ELSE
    P = 26.6 - 3.*X
  END IF
RETURN
END

C---
C UNFORMATTED DATA LINES:
C # OF DATA LINES(FIRST LINE, AN INTEGER)
CRUN#  T1      P2      DZDT      V      XWFMAS XWPMAS(ALL SUBSEQUENT LINES)
C
$ENTRY
23
2      37.5     30.      0.0496  10.     5.05    9.96
3      37.5     50.      0.0396  7.2     4.95    6.40
4      37.5     70.      0.0322  5.2     4.98    6.12
9      42.5     30.      0.0568  12.0    4.95    7.16
10     42.5     50.      0.0593  6.      4.93    7.75
11     42.5     70.      0.0506  5.2     4.82    6.12
5      47.5     30.      0.0813  9.4     4.97    6.93
6      47.5     50.      0.076   6.8     4.98    6.70
8      47.5     50.      0.0675  8.      4.90    6.71
7      47.5     70.      0.0710  5.4     4.89    7.33
12     42.5     30.      0.0688  10.     0.21    0.25
13     42.5     30.      0.0717  11.5    0.28    0.82

```



14	42.5	30.	0.0710	10.5	0.95	1.27
15	42.5	30.	0.0715	10.3	1.74	2.74
16	42.5	30.	0.0646	11.3	2.46	3.73
17	42.5	30.	0.0677	10.	3.35	5.0
18	42.5	30.	0.0653	11.5	4.30	5.86
19	42.5	30.	0.0633	11.	5.06	6.70
20	42.5	30.	0.0623	10.	6.14	8.37
21	42.5	30.	0.0578	11.	11.40	13.52
22	42.5	30.	0.0502	10.5	28.32	25.02
23	42.5	30.	0.0425	11.5	53.81	35.08
24	42.5	30.	0.0313	12.	73.19	45.5

LOX KIAEV

PA

EMERSON BOND

20% COTTON

Appendix D

Simulation Program Listing with  
Sample Output



C NOMENCLATURE  
C \*\*\*\*\*  
C  
C AC HEAT EXCHANGE AREA OF CONDENSER, SQ FT  
C AM MEMBRANE AREA, SQ FT  
C AR HEAT TRANSFER AREA -- REBOILER, SQ FT  
C AT CROSS-SECTIONAL AREA OF COLUMN, SQ FT  
C B INTERCEPT, RMIN EQUATION  
C B1, B2 COLUMN BOTTOMS FLOW RATE  
C CAP1, CAP2 ANNUALIZED CAPITAL COST, COLUMN 1, COLUMN 2, \$  
C CC1WOR TOT ANNUAL COST COL1 PRODUCING 190 PF, NO RECYCLE, \$  
C CCAP ANNUALIZED CAPITAL COST -- COLUMN, \$/YR  
C CCAPPV ANNUALIZED CAPITAL COST, PERVAPORATOR SECTION, \$  
C CCOL INSTALLED COST -- TOWER AND INTERNALS, \$  
C CCOND INSTALLED COST -- CONDENSER, \$  
C CCW ANNUAL COST -- COOLING WATER, \$/YR  
C CFEHE ANNUALIZED CAPITAL COST, FEED EFFL HEAT EXCH, \$  
C CINT INSTALLED COST -- TOWER INTERNALS, \$  
C CMU INSTALLED COST -- MEMBRANE UNIT, \$  
C CNRG ANNUAL ENERGY COST -- COLUMN, \$/YR  
C CP HEAT CAPACITY, BTU/(LBMOL\*DEG F)  
C CPCW HEAT CAPACITY -- COOLING WATER, BTU/(LB\*DEG F)  
C CPG UPGRADING COST PER GALLON, \$/GAL PRODUCT  
C CREB INSTALLED COST -- REBOILER, \$  
C CREF REFRIGERATION COST, \$/YR  
C CRF INSTALLED COST -- REFRIGERATION UNIT, \$  
C CSTM ANNUAL COST -- 25 # STEAM, \$/YR  
C CT TEMPERATURE CORRECTION TERM -- MEMBRANE FLUX MODEL  
C CTWR INSTALLED COST -- TOWER, \$  
C D1, D2 COLUMN OVERHEAD FLOW RATE, KMOL/HR  
C DELT TEMPERATURE DROP ACROSS MEMBRANE, DEG F  
C DHVAP HEAT OF VAPORIZATION, BTU/LBMOL  
C DHVC HEAT OF VAPORIZATION -- CONDENSER, BTU/LBMOL  
C DHVR HEAT OF VAPORIZATION AT REBOILER CONDITIONS, BTU/LBMOL  
C DHVS HEAT OF VAPORIZATION -- 25# STEAM, BTU/LB  
C DIAM DIAMETER -- COLUMN, FT  
C DOPT1, DOPT2 DIAMETER OF OPTIMUM COLUMNS 1, 2, FT  
C DT DELTA T ACR HT EXCHR OR COOLING WTR TEMP RISE, DEG F  
C DTCOND DELTA T ACROSS PERMEATE CONDENSER, DEG F  
C DTLM LOG MEAN TEMPERATURE DIFFERENCE, DEG F  
C EMV MURPHREE STAGE EFFICIENCY  
C ENRG1, ENRG2 ANNUAL ENERGY COST, COLUMN 1, COLUMN 2, \$  
C F1, F2 COLUMN FEED RATE  
C FC GUTHRIE'S MATERIAL OF CONSTRUCTION FACTOR, STAINLESS ST  
C FDP FEED TO PERVAPORATOR, KMOL/HR  
C G MEMBRANE FLUX, KMOL/(SQ M\*HR) OR LBMOL/(SQ FT\*HR)  
C H HEIGHT OF TOWER, FT  
C L # OF THEORETICAL STAGES, BOTTOM OF COLUMN 1  
C LBOT LIQUID MOLAR FLOW, BOTTOM SECTION OF COLUMN, KMOL/HR  
C LMID LIQUID MOLAR FLOW, MIDDLE SECTION OF COLUMN, KMOL/HR  
C LTOP LIQUID MOLAR FLOW, TOP SECTION OF COLUMN, KMOL/HR  
C M # OF THEO STAGES, MIDDLE OF COL1 OR BOTTOM OF COL2  
C MG MEAN MOLECULAR WT OF VAPOR -- TOP OF COLUMN  
C N # OF THEO STAGES, TOP OF COLUMN OR # REAL STAGES IN COL



```

C NOPT1, NOPT2  NUMBER OF STAGES FOR OPTIMUM COLUMNS 1, 2
C NTHEO        # THEORETICAL STAGES IN COLUMN
C P            PERMEATE FLOW RATE, KMOL/HR
C P2          PERMEATE PRESSURE, MMHG ABS
C QC          CONDENSER LOAD, BTU/HR
C QR          REBOILER LOAD, BTU/HR
C R           REFLUX RATIO
C RHOG        DENSITY OF VAPOR -- TOP OF COLUMN, LB/CU FT
C RMIN1,RMIN2  MINIMUM REFLUX RATIO
C ROPT1, ROPT2 OPTIMUM REFLUX RATIO, COLUMN 1, COLUMN 2
C T1          AVERAGE TEMPERATURE OF FEED TO PERVAPORATOR, DEG C
C T1DEGF      AVERAGE TEMPERATURE OF FEED TO PERVAPORATOR, DEG F
C TAC         PLANT TOTAL ANNUAL COST, (= TCC + TEC), $
C TAC1, TAC2  TOTAL ANNUAL COST, COLUMN 1, COLUMN 2, $
C TACC1       TOTAL ANNUAL COST -- COLUMN 1 AT R, $
C TACC2       TOTAL ANNUAL COST -- COLUMN 2 AT R, $
C TACPVP      TOTAL ANNUAL COST, PERVAPORATOR, $
C TCC         TOTAL ANNUAL COST, COL1 + COL2 + PVP + FEHE, $
C TEC         TOTAL ENERGY COST, COL1 + COL2 + PVP, $
C TONS        TONS OF REFRIGERATION
C TPVP        TEMPERATURE OF PERVAPORATOR EFFLUENT, DEG F
C UC          OVERALL HEAT TRANSF COEF -- COND, BTU/(HR*SQ FT*DEG F)
C UCCW        UNIT COST -- COOLING WATER, $/MLB
C UCMU        UNIT COST -- MEMBRANE UNIT (INSTALLED), $/SQ FT
C UCREF       UNIT COST -- REFRIGERATION, $/(TON*DAY)
C UCS         UNIT COST -- 25 # STEAM, $/MLB
C UR          OVERALL HEAT TRANSF COEF -- REB, BTU/(HR*SQ FT*DEG F)
C V           VAPOR FLOW RATE, KMOL/HR OR LBMOL/HR
C VEL         VAPOR VELOCITY, FT/SEC
C WC          FLOW OF COOLING WATER, LB/HR
C WS          FLOW OF STEAM, LB/HR
C X           MOLE FRACTION ETHANOL IN LIQUID
C Y           MOLE FRACTION ETHANOL IN VAPOR
C XB1, XB2    COLUMN BOTTOMS COMPOSITION
C XB2W        MOLE FRACTION WATER IN STREAM B2
C XD1, XD2    COLUMN OVERHEAD COMPOSITION
C XD2W        MOLE FRACTION WATER IN STREAM D2
C XF1, XF2    COLUMN FEED COMPOSITION
C XF2W        MOLE FRACTION WATER IN STREAM F2
C XFDP        PERVAPORATOR FEED COMPOSITION
C XN, XM, XL  MOLE FRACTION ETHANOL IN LIQUID ON STAGE N, M, L
C XP          PERMEATE STREAM COMPOSITION
C YN, YM, YL  MOLE FRACTION ETHANOL IN VAPOR ON STAGE N, M, L
C ZM          SLOPE -- RMIN EQUATION
C
C *****
C INITIALIZE VARIABLES
C
C   DATA XF1, XB1, XB2 / 0.042, 0.0001, 0.995 /
C   DATA F1, B1, B2   / 1923.3, 1842.3, 81.0 /
C   FLOWS IN KMOL/HR FOR 10,000,000 GPY PLANT
C   XD1 = XFDP = XP = D1 = P = CAP1 = ENRG1 = TAC1 = ROPT1 = 0.0
C   DOPT1 = XD2 = XF2 = D2 = F2 = CAP2 = ENRG2 = TAC2 = ROPT2 = 0.0
C   NOPT1 = NOPT2 = 0

```



```

DOPT2 = FDP = T1 = P2 = CCAPPV = CREF = TACPVP = AC = CMU = 0.0
CRF = CFEHE = TCC = TEC = TAC = CPG = 0.0
C
C THIS ROUTINE WILL CALCULATE PLANT MASS BALANCES FOR A
C MEMBRANE-AIDED DISTILLATION SIMULATION FOR THE FOLLOWING INPUT:
C
C GIVEN: XF1, XB1, XB2, F1, B1, B2, MEMBRANE MODEL
C CHOSEN: FDP:P RATIO, XD1, XD2, XFDP
C
      J = 0
C
C FOR AN AVG FEED TEMP OF 41 DEG C, PERMEATE PRESSURE OF 30 MMHG,
      T1 = 41.0
      P2 = 30.0
C
C RATIO OF FDP TO P, RANGE 25 TO 50
DO 44 LL = 25, 50, 25
      RATIO = LL*1.0
C
DO 33 K = 888, 894, 2
      XD1 = K/1000.0
C
DO 22 JJ = 896, 902, 2
      XD2 = JJ/1000.0
C
DO 11 I = 901, 909, 2
      XFDP = I/1000.0
C
C MEMBRANE SELECTIVITY MODEL, UOP-TFC MEMBRANE, NEAR AZEOTROPIC FEED
      XP = 1.0 - 0.791*(1.0 - XFDP)**0.776
C
C PLANT MASS BALANCE EQUATIONS, KMOL/HR
      XF2 = (XFDP*RATIO - XP)/(RATIO - 1.0)
      D2 = (XB2 - XF2)/(XF2 - XD2)*B2
      F2 = D2 + B2
      D1 = (XP*B2 - XF1*F1 + XB1*B1)/(XP - XD1)
      P = B1 + D1 - F1
      FDP = RATIO*P
C
C IF A MASS BALANCE FOR THE CHOSEN PARAMETERS GIVES A NEGATIVE FLOW,
C SKIP OUT OF THE LOOP AND CHOOSE A NEW SET OF PARAMETERS.
      IF (D2.LT.0.01) GO TO 11
      IF (D1.LT.0.01) GO TO 11
      IF (F2.LT.0.01) GO TO 11
      IF (P.LT.0.01) GO TO 11
      IF (FDP.LT.0.01)GO TO 11
C
C THIS SECTION CALLS PRIMARY SUBROUTINES WHICH CALCULATE OPTIMUM
C PARAMETERS FOR EACH UNIT OPERATION.
C
      CALL SUBC1(XD1, XP, XF1, XB1, D1, P, F1, B1, CAP1, ENRG1, TAC1,
&              ROPT1, NOPT1, DOPT1)
      CALL SUBC2(XD2, XF2, XB2, D2, F2, B2, CAP2, ENRG2, TAC2,
&              ROPT2, NOPT2, DOPT2)

```



```

      CALL SUBPVP      (P,FDP,T1,P2,AC,CMU,CRF,CCAPPV,CREF,TACPVP)
C
C****  CALL INTER-UNIT HEATING AND COOLING SUBROUTINE
C      ESTIMATE COST OF INTERUNIT HEATING PER YEAR(+ OR - 25,000)
      CIUHE = 135000.0
C
C  ADD ANNUAL COSTS OF ALL UNITS TO GET PLANT TOTAL COSTS.
C
      TCC = CAP1 + CAP2 + CCAPPV + CIUHE
      TEC = ENRG1 + ENRG2 + CREF
      TAC = TAC1 + TAC2 + TACPVP
C
C  IN ORDER TO CALCULATE THE DIFFERENCE IN COST OF PRODUCING 200 PF ETOH
C  OVER THAT OF PRODUCING 190 PF ETOH, THE APPROXIMATE COST OF PRODUCING
C  190 PF (82.66 MOLE %) FROM 4.2 MOLE % FEED IS SUBTRACTED FROM THE
C  TOTAL ANNUAL PLANT COST.  THE COLUMN 1 MODULE WITHOUT THE RECYCLE
C  (C1WOR) PERMEATE WAS RUN WITH THE SAME FEED AS THE PLANT FEED AND
C  FOUND TO COST ABOUT $406,000 PER YEAR.
C  THE COST IS PRESENTED IN $/GAL PURE ETOH PRODUCED.  THEREFORE, FOR
C  A TEN MILLION GAL PER YEAR PLANT, COST PER GALLON (CPG) EQUALS THE
C  TOTAL PLANT ANNUAL COST MINUS $406,000 (COL1-- 190 PF) ALL DIVIDED
C  BY TEN MILLION GALLONS.  UNITS: ($/YR)*(YR/GAL) = $/GAL
C
      CC1WOR = 406000.0
      CPG = (TAC - CC1WOR)/10E+6
C
      J = J + 1
      RSPLT = (FDP - P - F2)/F2
C
C  PRINT SUMMARY
C  -----
C  PLANT
      PRINT910
910  FORMAT('  J    XD1    XD2    XFDP    XF2    D2      D1    P    FDP:P
      & R:F2    $CAP    $ENERGY $TOT ANNUAL    COST PER GALLON, $')
      PRINT91,J,XD1,XD2,XFDP,XF2,D2,D1,P,RATIO,RSPLT,TCC,TEC,TAC,CPG
91  FORMAT(I4, 3F7.3, F7.4, 3F7.0, 2F5.0, 3F12.0, F15.3)
C
C  COLUMNS
      PRINT400
400  FORMAT('  R1    N1  DIAM1    $CAP1    $ENERGY1    $TAC1',
      & 6X,'  R2    N2  DIAM2    $CAP2    $ENERGY2    $TAC2')
      PRINT40,ROPT1,NOPT1,DOPT1,CAP1,ENRG1,TAC1,
      &      ROPT2,NOPT2,DOPT2,CAP2,ENRG2,TAC2
40  FORMAT(F5.2,I5,F6.1,3F11.0,3X,F5.2,I5,F6.1,3F11.0)
C
C  PERVAPORATION SECTION
      PRINT600
600  FORMAT('  T1    P2    XFDP    FDP    $MEMBR    $CAP-REF',3X,
      & '$CAP    $ENR    $TAC-PVP')
      PRINT60,T1,P2,XFDP,FDP,CMU,CRF,CCAPPV,CREF,TACPVP
60  FORMAT(2F6.1,F8.4,F10.1,5F10.0)
      PRINT,('- -',MMM=1,22)
C

```







```

C FEED (FEED F1), AND THE PERMEATE RECYCLE STREAM (FEED P).
C
C A STAGE-TO-STAGE CALCULATION PROCEDURE IS USED, ANALOGOUS TO
C STEPPING OFF THE STAGES ON A MCCABE-THIELE DIAGRAM. CONSTANT
C MOLAL OVERFLOW IS ASSUMED.
C
C CALCULATION BEGINS FROM THE TOP OF THE COLUMN.
C THE ADJUSTABLE PARAMETER FOR THIS MODEL IS THE REFLUX RATIO, R
C
C LET R = 1.01*RMIN1 AND ITERATE TO ABOUT R = 1.3*RMIN1
  R = 1.01*RMIN1
  WHILE (R.LT.1.25*RMIN1) DO
C
  YN = XD1
  XN = XD1
C ASSUME ALL FEEDS SATURATED LIQUID.
  LTOP = R*D1
  LMID = LTOP + P
  LBOT = LMID + F1
  V = LTOP + D1
C
  L = M = N = 0
C TOP SECTION
  WHILE (XN.GT.XP) DO
    CALL F(XN, YN)
    N = N + 1
    YN = R/(R + 1.0)*XN + XD1/(R + 1.0)
  END WHILE
C
C MIDDLE SECTION
  XM = XN
  WHILE (XM.GT.XF1) DO
    YM = (LMID*XM + XD1*D1 - XP*P)/V
    CALL F(XM, YM)
    M = M + 1
  END WHILE
C
C BOTTOM SECTION
  XL = XM
  WHILE (XL.GT.XB1) DO
    YL = (LBOT*XL - XB1*B1)/V
    CALL F(XL, YL)
    L = L + 1
  END WHILE
  NTHEO = L + M + N
C
C -----> CAPITAL AND ENERGY COST ----- COLUMN 1 <-----
C
C THIS ROUTINE CALCULATES CAPITAL AND ENERGY COSTS FOR COLUMN 1 FOR
C A GIVEN REFLUX RATIO. GUTHRIE'S CORRELATIONS ARE USED AND
C UPDATED TO 1984 DOLLARS BY RATIO OF M&S VALUES 784/280 = 2.8
C CAPITAL COSTS ARE ANNUALIZED OVER SIX YEARS.
C
C VAPOR FLOW, STAGE EFFICIENCY--

```



C USING THE MURPHREE EFFICIENCY DATA ON ETHANOL/WATER FROM PERRY'S  
 C (REF. 32, FIG 18-25) IT WAS FOUND THAT A VAPOR VELOCITY OF 4.6 FT/S  
 C CORRESPONDED TO 77 PERCENT STAGE EFFICIENCY.

$$VEL = 4.6$$

$$EMV = 0.77$$

C AREA, DIAMETER OF TRAY

C CONVERT VAPOR FLOW RATE FROM KMOL/HR TO LBMOL/HR

$$V = V^*2.2046$$

C OTHER UNITS: MG, LB/LBMOL; RHOG, LB/CFRT; AT, SQ FT; DIAM, FT

$$MG = 43.0$$

$$RHOG = 0.0933$$

C DIVIDE BY 0.88 FOR DOWNCOMER, CONVERT SEC --> HR

$$AT = V^*MG / (RHOG^*VEL^*0.88^*3600.0)$$

$$DIAM = SQRT(4.0^*AT/PI)$$

C REAL TRAYS

$$N = NTHEO/EMV$$

C HEIGHT OF TOWER, 2 FT TRAY SPACING, FT

$$H = 2.0^*(N - 1) + 25.0$$

C INSTALLED COST, TOWER, FC REPR SS CLADDING

$$FC = 2.25$$

$$CTWR = 2.8^*101.9^*DIAM^*1.066^*H^*0.802^*(2.18 + FC)$$

C TOWER INTERNALS COST

$$FC = 2.7$$

$$CINT = 2.8^*4.7^*DIAM^*1.55^*H^*FC$$

C COLUMN CAPITAL COST

$$CCOL = CTWR + CINT$$

C-----

C CONDENSER

C CONDENSER LOAD

$$DHVC = 16700.0$$

$$QC = DHVC^*V$$

C AREA OF CONDENSER

$$DT = 66.0$$

$$UC = 150.0$$

$$AC = QC / (UC^*DT)$$

C INSTALLED COST, CONDENSER

$$FC = 2.81$$

$$CCOND = 2.8^*101.3^*AC^*0.65^*(2.29 + FC)$$

C COOLING WATER FLOW

$$CPCW = 1.0$$

$$DT = 30.0$$

$$WC = QC / (CPCW^*DT)$$

C ANNUAL COST COOLING WATER

$$UCCW = 0.075$$

$$CCW = WC^*UCCW^*0.959$$

C-----

C REBOILER

C REBOILER LOAD

$$DHVR = 17500.0$$

$$QR = DHVR^*V$$

C AREA

$$DT = 55.0$$

$$UR = 450.0$$

$$AR = QR / (UR^*DT)$$









```

ELSE
  PRINT, ' CHECK GRAPH OF VLE DATA FOR RMIN2 '
END IF
C SLOPE ZM
  ZM = (YD2W - YF2W)/(XD2W - XF2W)
  IF (ZM.LT.0.0) ZM = 0.0
C INTERCEPT B
  B = YD2W - ZM*XD2W
C RMIN2
  RMIN2 = XD2W/B - 1.0
C LET ABSOLUTE RMIN2 = 0.20 (CORRESPONDS TO 10% ENTRAINMENT)
  IF (RMIN2.LT.0.20) RMIN2 = 0.20
C
C-----
C THIS ROUTINE CALCULATES THE NUMBER OF IDEAL STAGES IN "COLUMN 2",
C A DISTILLATION COLUMN WITH ONE FEED, "F2". THIS
C FEED REPRESENTS THE PERMEATE STREAM FROM A PERVAPORATOR.
C
C A STAGE-TO-STAGE CALCULATION PROCEDURE IS USED, ANALOGOUS TO
C STEPPING OFF THE STAGES ON A MCCABE-THIELE DIAGRAM. CONSTANT
C MOLAL OVERFLOW IS ASSUMED.
C
C CALCULATION BEGINS FROM THE TOP OF THE COLUMN.
C
C THE ADJUSTABLE PARAMETER FOR THIS MODEL IS THE REFLUX RATIO, R
C LET R = 1.01*RMIN2 AND ITERATE TO ABOUT R = 1.4*RMIN2
  R = 1.01*RMIN2
  WHILE (R.LT.2.3*RMIN2) DO
    YN = XD2W
    XN = XD2W
C ASSUME ALL FEEDS SATURATED LIQUID.
    LTOP = R*D2
    LBOT = LTOP + F2
    V = LTOP + D2
C
    M = N = 0
C TOP SECTION
    WHILE (XN.GT.XF2W) DO
      CALL FTWO(XN, YN)
      N = N + 1
      YN = R/(R + 1.0)*XN + XD2W/(R + 1.0)
    END WHILE
C
C BOTTOM SECTION
    XM = XN
    WHILE (XM.GT.XB2W) DO
      YM = (LBOT*XM - XB2W*B2)/V
      CALL FTWO(XM, YM)
      M = M + 1
    END WHILE
    NTHEO = M + N
C
C -----> CAPITAL AND ENERGY COST SECTION -- COL2 <-----
C

```



```

C THIS ROUTINE CALCULATES CAPITAL AND ENERGY COSTS FOR COLUMN 2 FOR
C A GIVEN REFLUX RATIO. GUTHRIE'S CORRELATIONS ARE USED AND THE
C CAPITAL COSTS ARE ANNUALIZED OVER SIX YEARS.
C
C VAPOR FLOW, STAGE EFFICIENCY
C USING THE MURPHREE EFFICIENCY DATA ON ETHANOL/WATER FROM PERRY'S
C (REF. 32) IT WAS FOUND THAT A VAPOR VELOCITY OF 4.25 FT/S
C CORRESPONDED TO 77 PERCENT STAGE EFFICIENCY.
  VEL = 4.25
  EMV = 0.77
C AREA, DIAMETER OF TRAY
C CONVERT VAPOR FLOW RATE FROM KMOL/HR TO LBMOL/HR
  V = V*2.2046
C OTHER UNITS: MG, LB/LBMOL; RHOG, LB/CFWT; AT, SQ FT; DIAM, FT
  MG = 46.0
  RHOG = 0.0936
  AT = V*MG/(RHOG*VEL*0.88*3600.0)
  DIAM = SQRT(4.0*AT/PI)
C REAL TRAYS
  N = NTHEO/EMV
C HEIGHT OF TOWER
  H = 2.0*(N - 1) + 25.0
C INSTALLED COST, TOWER
  FC = 2.25
  CTWR = 2.8*101.9*DIAM**1.066*H**0.802*(2.18 + FC)
C TOWER INTERNALS COST
  FC = 2.7
  CINT = 2.8*4.7*DIAM**1.55*H*FC
C COLUMN CAPITAL COST
  CCOL = CTWR + CINT
C-----
C CONDENSER
C CONDENSER LOAD
  DHVC = 16750.0
  QC = DHVC*V
C AREA OF CONDENSER
  DT = 66.0
  UC = 150.0
  AC = QC/(UC*DT)
C INSTALLED COST, CONDENSER
  FC = 2.81
  CCOND = 2.8*101.3*AC**0.65*(2.29 + FC)
C COOLING WATER FLOW
  CPCW = 1.0
  DT = 30.0
  WC = QC/(CPCW*DT)
C ANNUAL COST COOLING WATER
  UCCW = 0.075
  CCW = WC*UCCW*0.959
C-----
C REBOILER
C REBOILER LOAD
  DHVR = 16670.0
  QR = DHVR*V

```





```

      X = ((Y - 0.0665)/0.8873)**(1.0/0.9533) + 0.06
    ELSE IF (Y.GE.0.0335) THEN
      X = ((Y - 0.0335)/1.1975)**(1.0/1.0246) + 0.03
    ELSE
      X = (Y/1.1081)**(1.0/0.9976)
    END IF
  RETURN
END

C
C *****
C 11111111111111111111-----111111111111111111111111
C 11111111111111111111 PERVAPORATOR SUBROUTINE 111111111111111111111111
C 11111111111111111111-----111111111111111111111111
C
      SUBROUTINE SUBPVP (P,FDP,T1,P2,AC,CMU,CRF,CCAPPV,CREF,TACPVP)
C
C THIS ROUTINE PERFORMS SIZE, COST, AND ENERGY COST CALCULATIONS
C FOR THE PERVAPORATION SECTION OF THE PLANT. THIS INCLUDES THE
C MEMBRANE MODULE SIZE AND COST, THE CONDENSER SIZE AND COST, THE
C THE DELTA T ACROSS THE MEMBRANE, TONS OF REFRIGERATION AND ITS
C COST, AND INSTALLED COST OF A REFRIGERATOR BASED ON THE CORRELATION
C IN PERRY'S, FIG. 25-5 (REF. 32), CORRECTED TO 1984 DOLLARS.
C THE CAPITAL COSTS ARE ANNUALIZED OVER 6 YEARS.
C
C FOR THE UOP-TFC MEMBRANE, CHOOSE T1= 41 DEG C, P2 = 30 MMHG
C FLUX THROUGH THE MEMBRANE FROM MODEL, KMOL/(SQM*HR)
  CT = (T1 - 42.5)/100.0*(1.0 + 0.3333*((P2 - 30.0)/40.0))
  G = 1.39E-4*EXP(0.0104*(760.0 - P2)) + CT
C CONVERT FLUX, G, TO LBMOL/(SQ FT*HR)
  G = G*0.2048
C
C AREA OF MEMBRANE, SQFT
  AM = P/G
C
C INSTALLED COST OF MEMBRANE MODULES AT $12./SQFT
  UCMU = 12.0
  CMU = UCMU*AM
C
C HEAT LOAD, Q, BTU/LBMOL, LATENT HEAT OF VAP AT 40 DEG C, BTU/LBMOL
  DHVAP = 18000.0
C Q PER LBMOL TOTAL THROUGHPUT
  Q = DHVAP*P/FDP
C
C CH IN TEMP BY SENS HEAT LOSS,DEG F; ADIABATIC SYSTEM
C CP(AZEO @ 40 DEG C)
  CP = 30.0
  DELT = Q/CP
C
C CONDENSER LOAD, QC, BTU/HR; TREFR TO 34 DEGF
C LET REFR TEMP = 1 DEG C = 34 DEG F
C FIRST CONVERT T1 DEG C TO T1DEGF
  T1DEGF = (T1 + 273.15)*1.8 - 460.0
C NOW TEMP OF PVP = T1DEGF - TEMP DROP FROM SENS HEAT LOSS
  TPVP = T1DEGF - DELT

```

```

C      DTCOND = TPVP - 34.0
C      AT T = 35 DEG C, DHVAP = 18200.0
C      DHVAP = 18200.0
C      QC = P*2.2046*(CP*DTCOND + DHVAP)
C
C      TONS OF REFRIGERATION NEEDED --- 1 TON = 12,000 BTU/HR
C      TONS = QC/12000.0
C
C      ENERGY COST OF REFR FROM REF. 33, CORRECTED TO 1984 $
C      UCREF = $1.60/(TON*DAY)
C      UCREF = 1.60
C      CONVERT TO $/YR... 8000HRS/(24HRS/DAY)
C      CREF = UCREF*(8000.0/24.0)*TONS
C
C      AREA OF CONDENSER, AC, SQ FT
C      FOR 10 DEGF DRIVING FORCE AND DELTA T REFRIGERANT = 10 DEG F
C      LOG MEAN DELTA T IS
C      DTLM = ((TPVP - 34.) - (34. - 24.))/ALOG((TPVP - 34.)/(34. - 24.))
C      LET UC = 150 BTU/(SQ FT*HR*DEG F)
C      UC = 150.0
C      AC = QC/(UC*DTLM)
C
C      CAPITAL COST CONDENSER, $
C      FC = 2.81
C      CCOND = 2.8*101.3*AC**0.65*(2.29 + FC)
C
C      INSTALLED COST REFR -- REF. 32 - FIG. 25-5 MODELED
C      CRF = EXP(0.654*ALOG(TONS) + 1.235)*1000.0
C      CORRECT TO 1984 DOLLARS
C      CRF = CRF*2.8
C
C      ASSUME VACUUM AND RECYCLE PUMP COSTS SMALL
C
C      ANNUALIZE CAPITAL COSTS OVER 6 YEARS, MEMBRANE COSTS OVER 3 YEARS
C      CCAPPV = (CCOND + CRF)/6.0 + CMU/3.0
C      ENERGY COST = CREF
C      TOTAL ANNUAL COST PERVAPORATION SYSTEM
C      TACPVP = CCAPPV + CREF
C
C      RETURN
C      END
C *****
$ENTRY

```



J	XD1	XD2	XFDP	XF2	D2	D1	P	FDP:P	R:F2	SCAP	SENERGY	\$TOT ANNUAL	COST PER GALLON, \$
46	0.892	0.898	0.901	0.9024	1724.	437.	356.	25.	4.	1304103.	4658265.	5827368.	0.542
R1	N1	DIAM1	\$CAP1	\$ENERGY1	\$TAC1			R2	N2	DIAM2	\$CAP2	\$ENERGY2	\$TAC2
4.06	123	14.0	539975.	2094630.	2634605.			0.20	59	14.6	374362.	1879845.	2254207.
T1	P2	XFDP	FDP	\$MEMBR	\$CAP-REF	\$CAP	\$ENR	\$TAC-PVP					
41.0	30.0	0.9010	8890.5	79978.	1037751.	254766.	683790.	938556.					

J	XD1	XD2	XFDP	XF2	D2	D1	P	FDP:P	R:F2	SCAP	SENERGY	\$TOT ANNUAL	COST PER GALLON, \$
47	0.892	0.898	0.903	0.9043	1157.	471.	390.	25.	7.	1323039.	4511853.	5699892.	0.529
R1	N1	DIAM1	\$CAP1	\$ENERGY1	\$TAC1			R2	N2	DIAM2	\$CAP2	\$ENERGY2	\$TAC2
4.04	116	14.5	545068.	2250434.	2795502.			0.44	76	13.1	371479.	1511606.	1883085.
T1	P2	XFDP	FDP	\$MEMBR	\$CAP-REF	\$CAP	\$ENR	\$TAC-PVP					
41.0	30.0	0.9030	9748.9	87700.	1102231.	271492.	749813.	1021305.					

J	XD1	XD2	XFDP	XF2	D2	D1	P	FDP:P	R:F2	SCAP	SENERGY	\$TOT ANNUAL	COST PER GALLON, \$
48	0.892	0.898	0.905	0.9063	860.	513.	432.	25.	10.	1342141.	4555674.	5762815.	0.536
R1	N1	DIAM1	\$CAP1	\$ENERGY1	\$TAC1			R2	N2	DIAM2	\$CAP2	\$ENERGY2	\$TAC2
3.96	119	15.0	576839.	2411725.	2988564.			0.68	75	12.2	338979.	1313593.	1652571.
T1	P2	XFDP	FDP	\$MEMBR	\$CAP-REF	\$CAP	\$ENR	\$TAC-PVP					
41.0	30.0	0.9050	10796.1	97121.	1178292.	291324.	830356.	1121680.					

J	XD1	XD2	XFDP	XF2	D2	D1	P	FDP:P	R:F2	SCAP	SENERGY	\$TOT ANNUAL	COST PER GALLON, \$
49	0.892	0.898	0.907	0.9083	679.	565.	484.	25.	14.	1367848.	4714971.	5947819.	0.554
R1	N1	DIAM1	\$CAP1	\$ENERGY1	\$TAC1			R2	N2	DIAM2	\$CAP2	\$ENERGY2	\$TAC2
3.92	112	15.7	587959.	2636003.	3223962.			0.87	83	11.4	329598.	1148153.	1477751.
T1	P2	XFDP	FDP	\$MEMBR	\$CAP-REF	\$CAP	\$ENR	\$TAC-PVP					
41.0	30.0	0.9070	12102.3	108871.	1269669.	315291.	930815.	1246106.					

J	XD1	XD2	XFDP	XF2	D2	D1	P	FDP:P	R:F2	SCAP	SENERGY	\$TOT ANNUAL	COST PER GALLON, \$
50	0.892	0.898	0.909	0.9103	556.	632.	551.	25.	20.	1388706.	5027711.	6281416.	0.588
R1	N1	DIAM1	\$CAP1	\$ENERGY1	\$TAC1			R2	N2	DIAM2	\$CAP2	\$ENERGY2	\$TAC2
3.92	98	16.6	584244.	2948525.	3532769.			1.02	92	10.7	324504.	1019549.	1344052.
T1	P2	XFDP	FDP	\$MEMBR	\$CAP-REF	\$CAP	\$ENR	\$TAC-PVP					
41.0	30.0	0.9090	13777.2	123938.	1381996.	344959.	1059637.	1404595.					

J	XD1	XD2	XFDP	XF2	D2	D1	P	FDP:P	R:F2	SCAP	SENERGY	\$TOT ANNUAL	COST PER GALLON, \$
51	0.892	0.900	0.901	0.9024	3191.	437.	356.	25.	2.	1409263.	6256807.	7531070.	0.713
R1	N1	DIAM1	\$CAP1	\$ENERGY1	\$TAC1			R2	N2	DIAM2	\$CAP2	\$ENERGY2	\$TAC2
4.06	123	14.0	539975.	2094630.	2634605.			0.20	44	19.8	479522.	3478387.	3957909.
T1	P2	XFDP	FDP	\$MEMBR	\$CAP-REF	\$CAP	\$ENR	\$TAC-PVP					
41.0	30.0	0.9010	8890.5	79978.	1037751.	254766.	683790.	938556.					



## Appendix E

## Ethanol/Water Vapor-Liquid Equilibrium Data



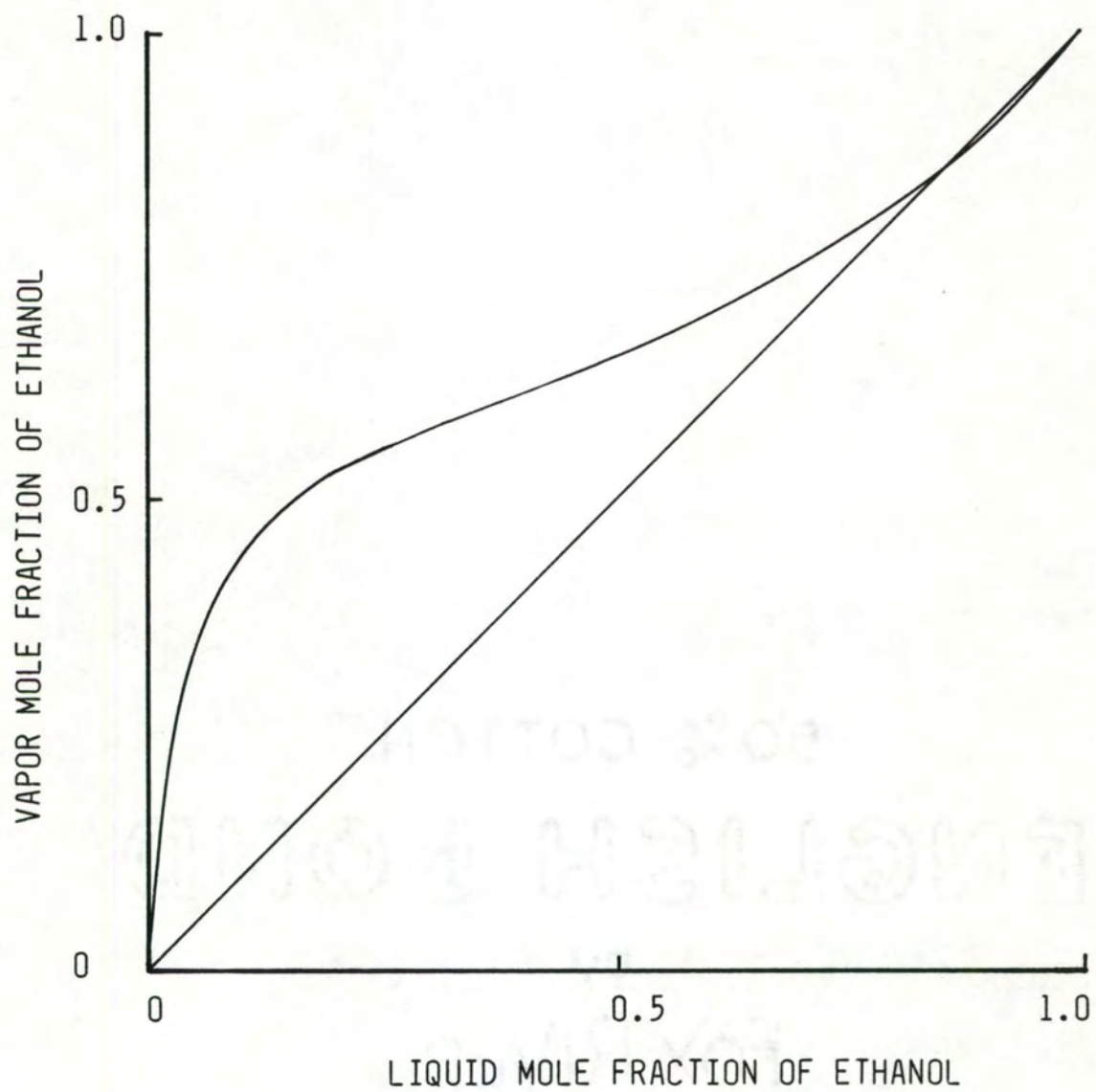


Figure E-1. Vapor-Liquid Equilibrium Curve for the Ethanol/Water System at 1 Atmosphere (15)

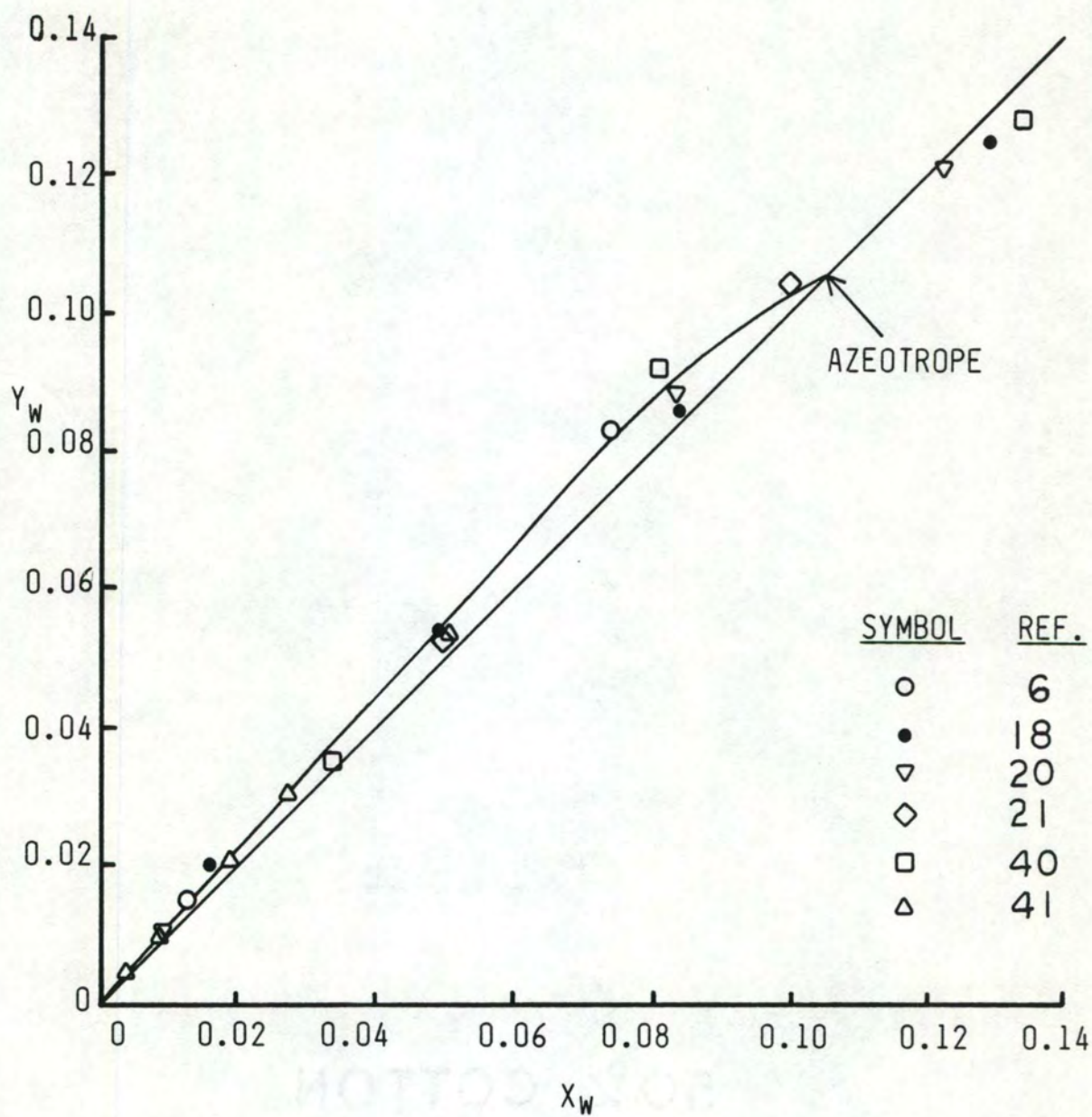


Figure E-2. Vapor-Liquid Equilibrium Curve for the Ethanol/Water System Below 15 Mole Percent Water



## Appendix F

## Cost Correlations

Utility costs used in the simulation program were \$0.075/Mgal for cooling water and \$2.60/Mlb for 25 psig steam.

Guthrie's Correlations (14) were used to calculate capital costs of the processing units. The equations used appear in the computer listing, Appendix D. The factor used to upgrade to 1984 dollars was the ratio of M&S values,  $784/280 = 2.8$ .

Refrigeration costs were computed by use of Peters and Timmerhaus (33, p. 881) and Perry (32, Figs. 18-25).

## Appendix G

## Nomenclature

$a_{1i}$	activity of species $i$ in the feed
$a_{2i}$	activity of species $i$ in the permeate
$b$	empirical constant for selectivity equation
$b_i$	empirical constant in diffusivity expression
$B_1$	column 1 bottoms flow rate
$B_2$	column 2 bottoms flow rate
$C_i$	concentration of species $i$ in polymer film
$C_{i,s}$	saturated concentration (solubility) of species $i$ in the polymer film
$C_T$	temperature correction term in the flux equation
$D_{oi}$	diffusion coefficient at dilute conditions
$D_c$	concentration-dependent diffusion coefficient
$D_1$	column 1 overhead flow rate
$D_2$	column 2 overhead flow rate
$F_1$	column 1 feed flow rate
$F_2$	column 2 feed flow rate
$F_{DP}$	pervaporator feed flow rate
$G_{TOT}$	total flux through membrane
$J_i$	Fick's Law flux of species $i$
$L$	active membrane thickness
$m$	empirical constant in selectivity equation
$P$	permeate flow rate
$P_1$	pressure on feed side of membrane
$P_2$	pressure on permeate side of membrane



$P_i^s$	saturated vapor pressure of species $i$
$P_{ref}$	an arbitrary reference pressure
$R$	universal gas constant; also pervaporator recycle stream flow
$T$	absolute temperature
$T_1$	pervaporator feed temperature
$T_{ref}$	an arbitrary reference temperature
$v_{1i}$	molar volume of species $i$ in feed
$v_{2i}$	molar volume of species $i$ in permeate
$x_{1i}$	mole fraction of species $i$ in liquid feed
$x_{2i}$	mole fraction of species $i$ in liquid permeate
$X_{B1}$	column 1 bottoms ethanol mole fraction
$X_{B2}$	column 2 bottoms ethanol mole fraction
$X_{D1}$	column 1 overhead ethanol mole fraction
$X_{D2}$	column 2 overhead ethanol mole fraction
$X_{F1}$	column 1 feed ethanol mole fraction
$X_{F2}$	column 2 feed ethanol mole fraction
$X_{FDP}$	pervaporator feed ethanol mole fraction
$X_p$	permeate mole fraction of ethanol
$x_w$	liquid mole fraction of water
$y_{2i}$	mole fraction of species $i$ in vapor permeate
$y_w$	vapor mole fraction of water
$z$	distance into membrane
$\alpha$	separation factor for preferred permeating species (water in this case)
$\alpha_{ij}$	separation factor for preferred permeating species $i$ in a binary mixture
$\gamma_{1i}$	activity coefficient of species $i$ in feed
$\gamma_{2i}$	activity coefficient of species $i$ in permeate

- $\mu_{i0}$  chemical potential of pure liquid  $i$  at  $T$  and  $P_{ref}$
- $\mu_{1i}$  chemical potential of species  $i$  in feed
- $\mu_{2i}$  chemical potential of species  $i$  in permeate
- $\pi_i$  osmotic pressure of species  $i$



#### LITERATURE CITED

1. Aptel, P., N. Challard, J. Cuny, and J. Neel, "Application of the Pervaporation Process to Separate Azeotropic Mixtures," *J. Membr. Sci.*, 1:271-87 (1976).
2. Aptel, P., J. Cuny, J. Jozefowics, G. Morel, and J. Neel, "Liquid Transport Through Membranes Prepared by Grafting of Polar Monomers onto Poly(tetrafluoroethylene) Films. I. Some Fractionations of Liquid Mixtures by Pervaporation," *J. Appl. Polym. Sci.*, 16:1061-76 (1972).
3. Aptel, P., J. Cuny, J. Jozefowics, G. Morel, and J. Neel, "Liquid Transport Through Membranes Prepared by Grafting of Polar Monomers onto Poly(tetrafluoroethylene) Films. II. Some Fractionations Determining Pervaporation Rate and Selectivity," *J. Appl. Polym. Sci.*, 18:351-64 (1974).
4. Binning, R. C. and R. J. Lee, "Separation of Azeotropic Mixtures," U. S. Patent No. 2,953,502, September 20, 1960.
5. Binning, R. C., R. J. Lee, J. F. Jennings, and E. C. Martin, "Separation of Liquid Mixtures by Permeation," *Ind. Eng. Chem.*, 53:45-60 (1961).
6. Bloom, C. H., C. W. Clump, and A. H. Koeckert, "Vapor-Liquid Equilibria and Latent Heats of Vaporization," *Ind. Eng. Chem.*, 53:829 (1961).
7. Brüscke, H. E. A., and G. F. Tusel, "Economics of Industrial Pervaporation Processes," presented June 1984 at the Membrane Conference, Stresa, Italy.
8. Gmehling, J. and U. Onken, Vapor-Liquid Equilibrium Data Collection, Dechema, W. Germany, 1977, Vol. 1, Part 1, pps. 150-196.
9. Gmehling, J. and U. Onken, Vapor-Liquid Equilibrium Data Collection, Dechema, W. Germany, 1981, Vol. 1, Part 1a, pps. 133, 154.
10. Gooding, C. H., "Reverse Osmosis and Ultrafiltration Solve Separation Problems," *Chemical Engineering*, 92:56-62 (1985).
11. Gooding, C. H. and F. J. Bahouth, "Membrane-Aided Distillation of Azeotropic Solutions," *Chem. Eng. Commun.*, (in press).



12. Greenlaw, F. W., W. D. Prince, R. A. Sheldon, and E. V. Thompson, "Dependence of Diffusive Permeation Rates on Upstream and Downstream Pressures, I. Single Component Permeant," *J. Membr. Sci.*, 2:141-151 (1977).
13. Greenlaw, F. W., R. A. Sheldon, and E. V. Thompson, "Dependence of Diffusive Permeation Rates on Upstream and Downstream Pressures, II. Two Component Permeant," *J. Membr. Sci.*, 2:333-48 (1977).
14. Guthrie, K. M., Process Plant Estimating, Evaluation and Control, Craftsman Book Co., Solana Beach, CA, 1974.
15. Hatch, L. F., Ethyl Alcohol, Enjay Laboratories, New York, 1962.
16. Hoover, K. C. and S. T. Hwang, "Pervaporation by a Continuous Membrane Column," *J. Membr. Sci.*, 10:253-71 (1982).
17. Huang, R. Y. M., and N. R. Jarvis, "Separation of Liquid Mixtures by Using Polymer Membranes. II. Permeation of Aqueous Alcohol Solutions Through Cellophane and Poly(vinyl Alcohol)," *J. Appl. Polym. Sci.*, 14:2341-56 (1970).
18. Johnson, A. I. and W. F. Furter, "Salt Effect in Vapor-Liquid Equilibrium. Part I.," *Can. J. Technol.*, 34:413 (1957).
19. King, C. J., Separation Processes, McGraw-Hill, New York, 1971, pps. 546-48.
20. Kojima, K., K. Ochi, and Y. Nakazawa, "Relationship Between Liquid Activity Coefficient and Composition for Ternary Systems," *Int. Chem. Eng.*, 9:342 (1969).
21. Kojima, K., K. Tochigi, H. Seki, and K. Watase, *Kagaku Kogaku*, 32:149 (1968). (Title not available; Secondary reference cited in Ref. 9, p. 133).
22. Madewell, C., TVA, Personal Communication, February 21, 1985.
23. Mehta, G. D., "Comparison of Membrane Processes with Distillation for Alcohol/Water Separation," *J. Membr. Sci.*, 12:1-26 (1982).
24. Mellan, I., Source Book of Industrial Solvents, Vol. III: Monohydric Alcohols, Reinhold, New York, 1959, pps. 99, 115.
25. Mokhtari-Nejad, E. and W. Schneider, "Industrial Separation of Azeotropic Mixtures by Pervaporation," presented June 1984 at the Membrane Conference, Stresa, Italy.



26. Mulder, M. H. V., "Pervaporation Separation of Ethanol-Water and of Isomeric Xylenes," PhD. Thesis, Ch. 7, Twente University of Technology, The Netherlands.
27. Mulder, M. H. V., J. O. Hendrikman, H. Hegeman, and C. A. Smolders, "Ethanol/Water Separation by Pervaporation," *J. Membr. Sci.*, 16:269 (1983).
28. Nagy, E., O. Borlai, and A. Ujhidy, "Membrane Permeation of Water-Alcohol Binary Mixtures," *J. Membr. Sci.*, 7:109-18 (1980).
29. Neel, J., Q. T. Nguyen, R. Clement, and L. Le Blanc, "Fractionation of a Binary Liquid Mixture by Continuous Pervaporation," *J. Membr. Sci.*, 15:43-62 (1983).
30. "1983 Annual Book of ASTM Standards, Vol. 15.05: Engine Coolants; Halogenated Organic Solvents; Industrial Chemicals," Designation E203-75 (reapproved 1981), pps. 304-13.
31. Paul, D. R., and J. D. Paciotti, "Driving Force for Hydraulic and Pervaporative Transport in Homogeneous Membranes," *J. Polym. Sci.*, 13:1201-14 (1975).
32. Perry, R. H. and C. H. Chilton, editors, Chemical Engineers' Handbook, 5th Ed., 1973, chs. 18 (Fig. 18-25), 25.
33. Peters, M. S. and K. D. Timmerhaus, Plant Design and Economics for Chemical Engineers, 3rd Ed., McGraw-Hill, New York, 1980, pp. 718-20, 881.
34. Rautenbach, R., and R. Albrecht, "Separation of Organic Binary Mixtures by Pervaporation," *J. Membr. Sci.*, 7:203-23 (1980).
35. Reid, R. C., J. M. Prausnitz, and T. K. Sherwood, The Properties of Gases and Liquids, 3rd Ed., McGraw-Hill, New York, 1977.
36. Riley, R. L., UOP Inc., Fluid Systems Division, San Diego, CA, Personal Communication, Nov. 7, 1984.
37. Schissel, P. and R. A. Orth, "Separation of Ethanol-Water Mixtures by Pervaporation Through Thin Composite Membranes," SERI/TP-255-1705 preprint, January 1983.
38. Sheldon, R. A. and E. V. Thompson, "Dependence of Diffusive Permeation Rates on Upstream and Downstream Pressures, III. Membrane Selectivity and Implications for Separation Processes," *J. Membr. Sci.*, 4:115-27 (1978).
39. Tusel, G. and A. H. Ballweg, "Method and Apparatus for Dehydrating Mixtures of Organic Liquids and Water," U. S. Patent Application No. 4,405,409, September 20, 1983.



40. Van Zandijcke, F. and L. Verhoeye, "The Vapor-Liquid Equilibrium of Ternary Systems with Limited Miscibility of Atmospheric Pressure," *J. Appl. Chem. Biotechnol.*, 24:709 (1974).
41. Vostrikova, V. N., M. E. Aerov, R. E. Gurovich, and R. M. Solomatina, *Zh. Prikl. Khim.*, 40:683 (1967). (Title not available; Secondary reference cited in Ref. 9, p. 154).